

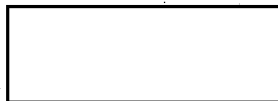
Declass Review by NIMA/DOD

STATINTL

FINAL REPORT

- of -

Contract



STATINTL

FEASIBILITY STUDY TO DETERMINE THE UTILIZATION
OF A DIPOLAR SUSPENSION FOR A LIGHT AMPLIFYING SCREEN

--

Period from March 1, 1965 to August 31, 1965



STATINTL

TABLE OF CONTENTS

<u>Section</u>	<u>Page</u>
I INTRODUCTION	
A. Foreword	1
B. Background	4
C. Concepts	4
D. The Photoion Dipole Effect	4
1. The Single Layer Photoion-Dipole Suspension	4
2. The Single Layer Photodipole Suspension	6
3. The Two-Layer Photoion-Dipole Suspension	7
4. Two-Layer Photoconductive Rod Matrix Layer and Dipole Layer	7
5. Oriented Photoconductive Dipole Layer	8
E. Dipole Materials	9
F. Photodipolar Materials	9
G. Photoion References	10
II PHOTOION DIPOLE	
A. The Photoion Effect	1
B. Mathematical-Physics of the Photoion Effect	6
(a) Introduction	6
(b) Ion Mobility - Table	8
(c) Symbols	9
(d) Operating Conditions and Equations	12
(e) Examples	28
C. Experimental Work	
1. Work Program	36
2. Equipment	38
3. Test Results	42
D. Conclusions	53
E. Further Work Program	55
III PHOTODIPOLES	
A. Object	1
B. Discussion	1
C. Photodipolar Materials	3
D. Experimental Work	3
E. Mathematical-Physics	5
(a) Symbols	5
(b) Equations	6
(c) Example	7
F. Conclusions	8
G. Further Work Program	8

TABLE OF CONTENTS (2)

<u>Section</u>	<u>Page</u>
IV PHOTOCONDUCTIVE ROD MATRIX LAYER	
A. Objects	1
B. Description	1
C. Materials	2
D. Mathematical-Physics	
(a) Symbols	3
(b) Equations	3
E. Experimental Work	
(a) Work Program	5
(b) Test Results	7
F. Conclusions	9
G. Further Work Program	10
V ORIENTED DIPOLE PHOTOCONDUCTIVE LAYER	
A. Description	1
B. Discussion	2
C. Further Work Program	3
VI QUESTIONS AND ANSWERS	
VII REFERENCES	
VIII FIGURES	
IX APPENDIX	
A. Proposal	
B. Questions	
C. VARAD	
D. TECOM Films	

STATINTL

TAB

I INTRODUCTION

A. Foreword

STATINTL
STATINTL
This is a Final Report on work performed on our Project [] covering period from March 1, 1965 to August 31, 1965, in accordance with our Proposal [] Appendix A herewith.

STATINTL
The objective of the present contract is to determine the feasibility of utilizing a dipolar suspension in the development of an advanced rear projection screen or light amplifier. To aid in making this determination, certain questions were propounded which are set forth in Appendix B herewith.

STATINTL
In our Proposal [] bottom of page 4, our Work Program was divided into two phases as follows:

Phase I will include the studies of the dipolar photoionic phenomena to establish the necessary parameters.

Phase II will comprise the construction and test of a system shown in Figure 1.

On page 5 it is stated that the work on Phase I will continue for six months, but it is hoped that at the end of four or five months progress will be sufficient to make a demonstration based on Figure 1.

In the course of the present program, an initial period of about three months was required to assemble the electronic equipment and make it operational, run initial tests and educate the project personnel.

A literature survey of photoion materials was made. Sources of supply for certain available photoionic materials

were located and many of these materials were acquired in readiness for our tests.

To establish a theoretical basis for the experimental study of the photoionic dipolar effect, a mathematical-physics study was commenced and completed.

Only about two months were left for actual experimental studies of the photoionic effect. The photoionic effect was discovered as predicted. The experimental data shows that the order of magnitude of the discovered photoion effect is in accord with theoretical predictions. It was shown that ultraviolet light decreases the initial applied electric field intensity across a photoion layer, to approximately zero. It was predicted that dipolar particles suspended in the photoion layer would be modulated by the incident ultraviolet light intensity because of the corresponding decrease in the electric intensity across the layer. This modulation effect was also observed on the last days work on the program.

Concurrently with the above work, certain approaches for accomplishing the same result were briefly investigated. These other approaches are considered in Sections III, IV and V.

Thus, the photoion effect and the photoion-dipolar effect have been shown to exist. These effects constitute a new large branch of Electro-optics, and experimental work on this problem can only be said to have commenced.

The work on the initial Phase I evidently could not be completed in terms of available time and money. Phase I

should, therefore, be extended for at least another six months and funded for this period to experimentally determine the parameters for an optimum photoion dipolar combination.. When this information is available, Phase II can be undertaken.

It is premature to fully answer all of the questions in Appendix B. However, the answers to the questions in Section VI are based upon present state of the theoretical and experimental knowledge gained thus far on this project. Some of the questions are definitely answered. The answer to the other questions can only be given after further work.

B. Background

The background literature on photoions is given in Part G of this Section.

The photoion dipolar concept developed as a result of the familiarity of the personnel [REDACTED]

[REDACTED] with both concepts, led to a proposal (Appendix A) which resulted in this contract.

The historical development of the dipolar concept presently known as VARAD is treated in Appendix C.

C. Concepts

The photoion dipolar screen combines two separate concepts:

(1) Dipole Effect - Control of light by the orientation of dipoles.

(2) Photoion Effect - Photoions produced by uv light are separated electrically, and modify the electric field.

(3) Coupling effects (1) and (2).

D. The Photoionic Dipole Effect

A coupling of the photoionic effect and the dipole effects, using a uv image to modulate visible light by changing the orientation of the dipoles, may be accomplished by:

(1) The Single Layer Photoion-Dipole Suspensions

The dipole suspension and photoions are present in a single fluid layer and the photoions influence the orientation of the dipoles in an electric field. The photoions are separated to more or less shield the applied electric field

causing the orientation of the dipoles within the layer to be modulated by the presence of the uv image.

In a single layer photoion-dipole suspension, the compatibility of the dipole and the photoionic solute must be considered. These must not react chemically, which might cause a degradation, or a lessening of the efficiency of either the photoionic solute or the dipole suspension.

Examples of chemically inert dipoles are (a) dipolar metallic rods such as chromium-dipole rods; and (b) metal vapor coated submicron alumina or silica monoxide whisker filaments. Work on these inert dipolar materials is presently being undertaken.

Consider a fluid layer containing a photoion solute and metal dipoles in suspension. When an ultraviolet light pulse arrives, positive and negative ions are produced within the fluid. If also an electric field is applied, the metallic dipoles take on induced positive and negative charges at opposite ends, and the photoions move to neutralize the charged ends of the dipole. An electric current passes through the metal dipole as the ions discharge the ends of the dipoles. Photoions will decrease in number and, therefore, fewer will be available to travel to the opposite faces of the VARAD cell to neutralize the electric field.

Thus the presence of metallic dipoles will have an effect similar to that of increasing the recombination rate of the dipoles and will tend to reduce the magnitude of the

shielding effect. This effect will tend to become more pronounced for high concentrations of dipoles. In dilute suspensions where the dipoles are far apart, there will be less tendency for this effect to occur. At the same time the discharge of the charged ends of the dipole will decrease the turning torque which is equivalent to the shielding effect.

On the other hand, with dielectric dipoles, no current passes through the dipoles. The photoions neutralize the induced potential on the dipole and prevent the dipoles from reacting with the electric field. With dielectric dipoles it may not be necessary to depend upon the shielding of the internal electric field by charge separation to the surfaces of the photoion-dipole layer. Shielding will occur on the induced charges of the dipoles by the attachment of available local photoions. This produces a more rapid and complete shielding.

There will be an upper limiting frequency to dipole ion shielding effect because the mobility of the ions is small. The AC field reversal is too rapid, the photoions cannot move towards and away from the dipole ends quickly enough to shield effectively.

2. The Single Layer Photodipole Suspension

The dipoles in suspension in a single fluid layer are photodipoles whose conductivity varies with the intensity of the incident light, thereby directly controlling the orientation in an ultrahigh frequency alternating electric field. The photodipole includes both the photoion effect and the dipole

effect in a single particle. This is the most sophisticated and preferred method.

(3) The Two-layer Photoion/Dipole Suspension

The photoion solute is contained in one layer, and the dipole suspension is in a second layer. The two layers are separated by a transparent insulating sheet. An electric field is applied across both layers. When the transparent photoion layer is illuminated, ions separate. The change in the electric field is induced by the motion and separation of charges in the photoion layer. As the electric field strength across the dipole layer is increased, the dipoles increase their orientation.

(4) Two-Layer Photoconductive Rod Matrix Layer and Dipole Layer

This device is also a two-layer system. The photo-responsive layer is a solid state device comprising rods and photoconductive material held within the transparent matrix. When illuminated with uv light, the resistivity of the photoconductive rods is decreased and the voltage across the dipole layer is increased thereby increasing its transmission. This device presents fabrication engineering problems but its electro-optical characteristics can be predicted on the basis of engineering design.

5. Oriented Photoconductive Dipole Layer

This is also a solid state photoresponsive layer containing zinc oxide crystals embedded in the transparent matrix and permanently oriented normal to the layer surface. The resistivity of the zinc oxide crystals decreases when illuminated by uv light. If the accicular crystal is about $1/3$ of a wavelength of light in length and about $1/30$ of a wavelength of light in width, then visible light will be transmitted through the layer. Incident uv light will be absorbed where it passes through the zinc oxide crystals. The zinc oxide crystal is present in high concentration. It is a solid state device possessing no apparent graininess and thus high resolution is attainable with little or no degradation.

E. Dipole Materials

Dipoles may comprise:

- (1) Metallic (conducting)
- (2) Dielectric (non-conducting)
- (3) Semiconductors

These include dichroic crystal needles such as herapathite which contain linear polyiodide chains.

F. Photodipolar Materials

The photodipoles comprise semiconducting crystal-whiskers. Examples are:

(1) Photoconductive Whiskers - The conductivity of certain crystal whisker materials increases when illuminated with visible or ultraviolet light. For example:

(a) Silicon and germanium form crystal whiskers, the conductivity of which increases when illuminated with visible light.

(b) Zinc oxide forms crystal whiskers, the conductivity of which increases when illuminated with uv light.

(2) Photovoltaic Whiskers - These develop a potential difference along the whiskers when illuminated by ultraviolet light. As an example, zinc sulfide becomes conducting and photovoltaic when illuminated by uv light.

G. Photoion References

Various references relating to photoions are listed in Section VIII. These references have been reviewed for their pertinence to the present project.

Photoions may be produced from polymers¹.

Photovoltaic solar energy converters² rely upon the production of photoions. In reference 2, Figure 1, there is shown electron hole pairs in semiconductors with various energy gaps starting with 2.25 electron volts. In each case the number of electron hole pairs generated is obtained under the assumption of the existence of an abrupt absorption edge with complete absorption on the high energy side. For example, for the energy spectrum of the sun on a bright, clear day at sea level, an energy gap of 2.25 electron volts corresponds to approximately 0.53 microns wavelength. At shorter wavelengths than this down to 0.3 microns in the ultraviolet, approximately 5.8×10^{16} electron hole pairs/cm²-sec are generated by sunlight.

The number of electron hole pairs generated due to ultraviolet light from 0.3 to 0.4 microns, which includes most of the ultraviolet spectrum of the sun, is of the order of $N = 10^{16}$ electron-hole pairs/cm²-sec which can be used as a measure of comparison for ultraviolet flux.

An estimate of the expected efficiency of conversion of the photon energy to electron hole pairs for the quantum efficiency, may be obtained from this reference. For example, Figure 14 of this reference shows that for an energy gap of 3 or 3.5 electron volts corresponding to the ultraviolet light of an average wavelength of about 0.37 microns, the collection efficiency is of the

order of 75 to 80% with two trap levels and about 50% with 1 trap level in the forbidden gap.

A photovoltage has been observed at the interface between germanium and electrolyte³. This observation may have a bearing on the production of photodipoles, discussed in Section III.

There are many studies of the role of light in photosynthesis. Interesting summaries of the work in this field and a bibliography are given in references 4 and 5. In photosynthesis there are chemical structures which convert light photon energy to electrical charges which are then utilized to produce chemical changes. Possibly some of these compounds or their homologues may be used to produce photoions.

There are many simple substances which produce photoions. One such is hydrogen iodide^{6,7}.

The quantum yield was determined for the wavelengths 2070, 2530 and 2820Å, and found to be approximately 2, and also found to hold for wavelengths slightly greater than 3,000Å.

CsPbX₃-crystals⁸ with perovskite structure are photoconductive, CsPbCl₃ having its maximum spectral sensitivity in the violet, CsPbVr₃ in the blue to green region and CsPbI₃ in the red region, that is the spectral region which is complementary to the colour of the crystals.

Certain crystals such as anthracene⁹ may absorb a photon and send an electron into the solution leaving a mobile hole in the crystal which can move through the crystal to the opposite crystal face to be discharged. It is shown that small amounts of certain dyes dissolve in the solution and sensitize the photoconduction of the anthracene on the positive side, there being no effect on the negative side. Various dyes such as fluorescein have the

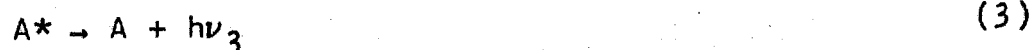
Approved For Release 2002/06/17 : CIA-RDP78B04747A002500040003-8
 sensitive property. The results of these experiments are given in the graph Figure 3 p. 308 of the reference. This reference also states the conclusion on p. 309 as follows:

"In conclusion it seems that for all observed effects of the dye (the increase in i_+ and i_- in the absorption region of anthracene and also the generation of a new photo-sensitive region at longer wavelengths) the dye has to be electronically excited. As outlined above this may happen in three ways: D = dye; A = anthracene; A*, D* denote excited singlet states):

I) by absorption of incident light:



II) by absorption of crystal fluorescence:



III) by radiationless energy transfer from the excited crystal:



In all three cases the excited dye subsequently abstracts an electron from anthracene (oxidation):



leading to mobile holes in the crystal observable as a current in the outer circuit.

The assumption that the dye acts in the same way in all three cases is further supported by the action of small amounts of iodine, which enhance the effect of the dye in all three cases.

In cases I and II the dye is (optically) excited to a singlet state and the same will therefore be true for the third case (energy transfer). This does not mean that the final reaction (electron transfer) takes place between the dye in its excited singlet state and the crystal. In fact it is well known that photochemical reactions with dyes often proceed through the excited triplet state of the dye. The positive effect of iodine on the dye sensitized photocurrent fits well into this scheme and can be interpreted as a result of an increased rate of singlet-to-triplet internal conversion of the dye induced by the heavy iodine molecules which are adsorbed together with the dye at the crystal surface."

Much of our work on the voltage divider effect (Section IV) was done with zinc oxide crystals. We have also proposed the use of zinc oxide crystals as possible photodipoles. Certain of the optical and electrical properties of zinc oxide crystals are given¹⁰ but pertinent information is lacking.

Dye sensitized photoresponse in organic semiconductors are described¹¹; in particular, there is described the organic photo-semiconductor copper phenylacetylide (PAC) and various dyes which are capable of photosensitizing this material.

An important reference¹² describes the photoelectric effects of polymers and their sensitizers by dopants. A most important finding shows that the presence of a donor (D) acceptor (A) interactions play a decisive role for the photo-induced generation of charge carriers according to:

light

$DA \rightleftharpoons D+A-$

(8)

p-Type conduction may be postulated with D-hosts are doped with A-impurities, which act as electron traps, and an exchange of positive charges (holes) between excess D molecules take place. In the reverse case n-type conduction with trapping of holes and migration of electrons may be postulated.

About 100 compounds are listed in this article and lists of donors and acceptor compounds are given. These are mostly multiple benzene ring compounds with various side constituents which render them either donor or acceptors. Many such compounds may be dissolved, and utilized in solution for the production of photoions. (See Section II)

There is a large patent literature¹³⁻²⁸ relating to photoconductive layers used for electrophotography. This literature contains abundant references to photoconductive polymeric compounds and dye-sensitizers therefor^{13,14}.

The known photosensitive chemical compounds, polymers and dye sensitizers form a fruitful field for the investigation of compounds which may prove suitable for the production of photoions. Several hundred compounds are listed in these references¹⁵⁻²⁸. In our experimental work, some of these (for example, polyvinyl carbazol), have proven to be suitable for the production of photoions. (Section II)

Reference 29 states:

"The absorption and reflection of radiation by an inorganic semiconductor may be enhanced by the choice of an ultraviolet absorber used in combination with the inorganic material. Resorcinol is an excellent ultraviolet-absorbing material, and in addition is an inexpensive, exceptionally stable material. Current theories predict that under excited conditions the resorcinol will absorb radiation in its characteristic absorption region and transmit the excitation to produce some free carriers in the photoconducting zinc oxide layer. Since we will initially have a minimum number of free carriers in the oxide layer, the excitation should shift the reflection edge into the visible region, without creating a reflection minimum."

The presence of resorcinol in the zinc oxide layer may increase the conductance of the layer.

Resorcinol should also be tried in the photoionic cell.

TAB

II PHOTOION DIPOLE

A. The Photoion Effect

Figure 2 shows a cross section of a cell adapted for displaying the photoionic effect. Ultraviolet light 7 is supplied in the form of a pulse 10 having a time duration t_1 and an intensity I_0 . It is assumed that the pulse is rectangular.

An electric pulse 8 is supplied starting at time t_2 and ending at time t_3 . This shows that the ultraviolet light pulse 10 and the electric pulse 8 need not have the same starting time nor the same time duration. Time is figured as 0 at the onset of the light pulse. At a time t_2 the voltage pulse starts. At a time t_1 the light pulse ends. At a time t_3 the voltage pulse ends. In certain cases it may be desirable to start the voltage pulse simultaneously with the light pulse in which case $t_2 = 0$.

Referring to Figure 3 the potential distribution across the space between the transparent electrodes 5 and 6 is shown. The electrode 5 is assumed to be at zero potential and the voltage pulse is applied to the electrode 6 with a positive potential. This causes the negatively charged particles 20 to be attracted toward the electrode 6 and the positively charged particles 21 attracted toward the grounded transparent electrode 5. The negative ions eventually are stopped at the surface BE. BE is the inner surface of the plate 3 which is coated with an increasing concentration of negative charges 22.

This will depress the potential from $V_{2,0}$ at B, to $V_{2,t}$ at E. In a similar manner positive charges 21 start coating the surface of the FC with positive charges 23 and thus increase the potential from $V_{3,0}$ at C, to $V_{3,t}$ at F. Thus the potential difference between the surfaces EB and FC will decrease. This is shown by the smaller slope of the line EF which means a decreased electric field intensity across the dipolar suspension, compared to the initially strong electric field gradient as shown by the greater slope of the line BC which corresponds to the initial electric intensity.

Owing to the motion of the charges, the negative charges 24 are distributed in space and the positive charges 25 are also distributed in space. However, since the mobility of the negative charges, particularly if they are free electrons instead of negative ions, is greater than that of the positive charges, there will be a different variation of negative space density than that of positive space charge density. In fact the buildup of negative charges on the surface BE will be more rapid than the buildup of positive charges on the surface FC, and the positive charges will remain distributed throughout the solution for a longer period of time than the negative charges.

Another factor influencing the unequal distribution of positive and negative charges across the distance from $Z = 0$ to $z = \infty$ is the exponential absorption of the ultraviolet light

In the dipole medium 30. Initial intensity at $z = 0$ is I_0 and the light intensity falls off to I_z at a distance z from the surface EB, as shown in Figure 3.

The light intensity varies exponentially from $z = 0$ to $z = d$. It is assumed that the plate 3 is of quartz and that attenuation of ultraviolet light is negligible therein.

It is also assumed that the dipole suspension 30 contains ultraviolet absorbing molecules which will produce at least 90 to 99% ultraviolet absorption. This is necessary in order to have an efficient utilization of the ultraviolet light intensity. In such case most of the photoions will be produced in the layers closest to the surface EB, and form few photoions in the dipolar suspension close to the surface FC.

Initially the positive and negative charges are equal in numbers in any given layer of solution and the space charge will be zero; hence, the potential distribution line BC will be a straight line as shown. The line FE is also straight when the positive and negative charges are entirely swept from the solution and deposited on the surfaces as charges 22 and 23 respectively. However, in the meantime the curve will be an S curve similar to that shown as EJKGF. Point G will not be equidistant between the surface EB and FC but closer to the surface EB.

The physical parameters of the problem can be assigned numerical values which are known from the literature. For example, a table of ionic mobilities is given in Section II-B(b).

Figure 2 shows a cross section of a photoion layer between laminated glass sheets, each laminate containing a transparent conducting layer.

Figure 3 shows the potential distribution across the space between the transparent electrodes of Figure 2.

Figure 4 shows that the ultraviolet pulse on the dipole cell layer is absorbed exponentially. The photoions initially have an exponential distribution in space.

Figure 5 shows dynamic conditions within a photoion layer. The charge density and velocity of positive and negative ions are shown entering and leaving a photoion layer of thickness Δz , at a distance z from one face of the photoion layer.

Figure 6 shows electric surface charge density and current density versus time in a photoion cell subjected to a square voltage pulse and a square uv light pulse.

Figure 7 shows the experimental setup for the study of the photoion effect.

Initially the capacitance per unit area of the system includes the photoion layer 1, and the two glass layers 2 and 3.

After the photoions have been formed, and migrate to the surfaces of the layer 1, the voltage field across 1 is cancelled and the entire voltage appears across the glass sheets 2 and 3. In effect, 1 has become a conductor. Because the capacitance per unit area increases from C_{11} to C_{12} , the charge per unit area on the transparent conductors 4 and 5 increases from Q_{11} to Q_{12} in the time t_0 required for the photoions to migrate to the surfaces of the layer 1.

It is assumed that a DC pulse is initially applied across the transparent conductive layers and that this DC pulse is not sufficient by itself to cause the photoions to break down. The DC pulse is applied for an initial period sufficient to establish a charge Q_{11} on the transparent conductors. At this point, a light pulse ϕ is applied. The light pulse as N photons which produce a sufficient number of photoions, so that when these migrate to the surface of the photoion layers, a zero field is established within the photoion layer.

In effect, the photoion layer is thus replaced by a conductor. Opposite charges now appear on both sides of the glass layers, and the maximum field is across the glass layers with no field across the photoion layer.

The photoionic solutes must not react with the herapathite or other dipole suspensions. It is preferable for the photoionic solute to be dissolved in the dipole fluid. However, in the event that there is a reaction, the tandem cell technique may be used.

B. MATHEMATICAL-PHYSICS OF THE PHOTOION EFFECT

(a) Introduction

A theoretical mathematical study is presented herein which is a result of several months of effort to consider the interrelationships of the parameters on the basis of known physical laws. These laws have been applied to the present problem and new equations interrelating the parameters have been derived. Now that these new equations are available, they have indicated a procedure for evaluating the parameters which are important to the photoion effect. Moreover, it now becomes possible to compare the experimental results with the order of magnitude of results predicted by theory. It is also now possible to identify the species of ion by actually measuring the mobility of the ions concerned.

With reference to the ion mobilities, the theory has been derived on the simplest basis and, therefore, must be considered to be only a first approximation. The actual observed variations will probably be more complicated than those which have been predicted on the simple assumptions herein made because, in general, there will be a positively charged ion and a negatively charged ion and their mobilities are usually different, in some cases by several orders of magnitude, depending upon the chemical nature of the photoion.

In the search for species of photoions which may prove useful for this effect, these may be compared with the standards herein derived to enable a choice to be made amongst

the various available materials which will be studied in the course of this work.

This study has determined the relationship between the following parameters concerned with photoion effect:

1. Ion Velocity
2. Quantum Efficiency
3. Concentration of Photoion Molecules
4. Photoion Molecules/Unit Area
5. Initial and Final Capacitance/Unit Area
6. Initial and Final Surface Charge Density
7. Initial Voltage Across the Photoion Layer
8. Photoion Pulse Duration
9. Photoion Pulse Current Density
10. Photoion Mobility
11. Extinction Constant of Photoion Solute
12. Proportion of Photoion Solute Molecules Ionized

(b). ION MOBILITYUnits of Mobility k

$$1 - \overset{\text{cgs}}{\text{cm}^2/\text{volt-sec.}} = \overset{\text{mks}}{10^{-4} \text{ m}^2/\text{volt-sec.}}$$

TABLE
ION MOBILITY

Ion	$\overset{k}{\text{m}^2/\text{volt-sec.}}$ 10^{-8}
H ⁺	32.0
OH ⁻	18.1
Cl ⁻	6.9
K ⁺	6.6
Li ⁺	3.6
Cu ⁺⁺	3.1

Δ Reference - Getman p. 484

-9-

(c) Symbols

All units are mks, except as noted.

a_g	=	thickness of glass layer - m
a_p	=	thickness of photoion layer - m
α	=	$(C_p/C_{12}) = (C_p/C_g)$
R	=	$1/(1 + \alpha)$
C_p	=	initial capacitance/m ² of photoion layer farads/m ²
C_{11}	=	initial capacitance/m ² of the cell farads/m ²
C_{12}	=	final capacitance/m ² of the cell farads/m ²
C_g	=	capacitance/m ² of the glass layers farads/m ²
C_s	=	concentration of solute in gms/cm ³
E	=	electric intensity volts/m
E_p	=	initial electric intensity in photoion layer volts/m
e	=	charge on the electron = 1.60×10^{-19} coulombs
ϵ_g	=	dielectric constant of glass layer
ϵ_o	=	8.85×10^{-12} farads/m
ϵ_p	=	dielectric constant of photoion layer
ϵ_s	=	extinction constant of photoion solute to uv light
h	=	Plancks Constant = 6.6256×10^{-34} joule sec
i	=	current density - amps/m ²
k	=	mobility in m ² /volt sec. See Table
m	=	molecular weight
M	=	mass per unit area of active absorber (photoion solute)
N_o	=	incident photons/m ² in uv light pulse
\dot{N}	=	light intensity of the light pulse in photons/m ² -sec
N_s	=	photons/gm of photoion solute
N	=	incident photons/m ² in uv light pulse at distance z into photoion layer

- n = number of solute molecules/ m^3
 n_o = Avagadros Number = 6.02×10^{23} molecules/gm mol
 n_s = number of solute molecules/ m^2 in the photoion layer
 n = number of electron charges/ m^3 produced by a light pulse
 n_p = electron charges/ m^2 produced by light pulse in the photoion layer = $n a_p$
 p = proportion of photoion solute molecules which are ionized to photoions
 ρ = charge density - coulombs/ m^2
 Q_{11} = initial surface charge density on the transparent conductors coulombs/ m^2
 Q_{12} = final surface charge density on the transparent conductors coulombs/ m^2
 η = quantum efficiency = $p n_s / N$
 t = time, sec
 t_p = time duration of the light pulse
 t_o = time for an ion to travel a distance a_p in an electric field of intensity E_p
 u = velocity of ion m/sec
 V = total voltage across the transparent conductors - volts
 V_p = initial potential difference across photoion layer - volts
 V_g = initial potential difference across glass layer - volts
 z = distance from one plane of the photoion layer

The mks units are most compatible with electrical quantities. However, since the cgs units are presently used for chemical quantities, initial derivations will be made in the cgs system, and quantities essential for electrical calculations will be converted to mks units.

Both systems will be used and consistent equations will be derived as noted in each case.

(d) Operating Conditions and Equations

The initial conditions are:

(1) A square pulse of voltage V applied across the transparent electrodes.

(2) The time constant of the cell and the feeder circuit is short. As a result, the initial charge density Q_{11} is quickly established on the transparent electrodes.

(3) The light pulse produces μN photoions/ m^2 , which migrate to the fluid layer surfaces, and the surface charge density on the photoion layer increases from Q_{11} to Q_{12} cancelling the potential difference across the photoion layer.

A voltage V is applied across the glass and fluid layers. V_p is the initial voltage across the fluid layers and V_g is the initial voltage across the glass layers.

Referring to Figure 6, the light pulse forms photoions, which migrate with a velocity u in the electric field across the fluid. The electric potential difference across the photoion layer is initially V_p and decreases to zero as the photoions reach the layer surfaces and cancel the field in the fluid.

-13-

1. Ion Velocity

The initial instantaneous velocity of the ion is:

$$u = kE_p = k (V_p/a_p) \quad (1)$$

When equilibrium is established, the full voltage V is applied across the glass layers only, and the surface charge density Q_{12} cancels the electric field within the layer 1.

2. Quantum Efficiency

A light pulse of time duration t_p supplies N photons/cm². There are η molecules/cm³ capable of becoming photoions upon absorbing a photon, and ηa_p molecules/cm² in the photoion layer. The photons are absorbed with a quantum efficiency μ , by a proportion p of the layer of photoion solute molecules, producing n electrons and n positive ions, which constitute n electron charges/cm³; and $n a_p$ electrons/cm² in a photoion layer of thickness a_p :

$$\mu N = n a_p = p \eta a_p = p \eta_s \quad (2)$$

When the uv light pulse intensity is \dot{N} , and its time duration is t_p , and the photoion solute concentration c_s is such as to provide sufficient molecules to be ionized, these ions travel in the electric field and reach the photoion layer surfaces, thereupon causing substantial cancellation of the electric field within the photoion layer. From (2), the relation of the final surface charge

density Q_{12} to these variables is:

$$Q_{12} = e \mu N = e p n_s \quad (3)$$

The intensity of the light pulse is \dot{N} photons/cm²-sec:

$$\dot{N} = N/t_p \text{ quanta/cm}^2\text{-sec.} \quad (4)$$

Hence from (3) and (4):

$$Q_{12} = e \mu \dot{N} t_p \quad (5)$$

From (3)

$$n_s = Q_{12}/ep \quad (6)$$

From (2)

$$N = (p/\mu) n_s \quad (7)$$

The energy of uv light depends on the duration t_p of the uv flash of intensity \dot{N} :

$$N = \dot{N} t_p \quad (8)$$

To create the photoions, the uv flash must:

(a) be a short fraction of the voltage pulse

time t_o :

(b) a uv light of adequate intensity \dot{N} and time duration t_p is applied before the voltage pulse. This time t_p must be much shorter than the ion recombination rate. To assure this:

$$t_p \ll t_o \quad (9)$$

From (6) and (7):

$$N = (i/e\mu) VC_g \quad (10)$$

The quantum efficiency is:

$$\mu = VC_g/Ne \quad (11)$$

In equation (11) the terms VC_g are determined electrically. The term N may be determined by observing the response of a calibrated photoelectric cell to the intensity \dot{N} of the uv light flash, and the duration of the light flash t_p from equation (8). With this data the quantum efficiency may now be calculated using a light flash intensity \dot{N} and duration t_p such as to produce a zero voltage field within the photoion layer.

3. Photoion Molecules/Unit Area

The solute has a molecular weight m , and a solute concentration c_s . A mol is the molecular weight expressed in grams. Since r_o is in molecules/mol and c_s is commonly expressed as $\text{gms/cm}^3 = \text{gms/ml}$, the number of solute molecules n per cm^2 is:

$$n = (r_o/m)c_s \text{ (molecules/m}^3\text{)} \quad (12)$$

From (12) the number of molecules/ cm^2 capable of becoming photoions in a thickness a_p is:

$$n_s = (r_o/m) c_s a_p = (r_o/m)M \quad (13)$$

4. Photons

From (2) and (13), the number of photons/ cm^2 required is:

$$N = (r_o/m)(n/u)c_s a_p \quad (14)$$

The required photons/gm of photoion solute in the layer may be obtained from (14):

$$N_s = (N/c_s a_p) = (\eta_o/m)(p/u) \quad (15)$$

5. Concentration Solute

From (13):

$$c_s = (m/\eta_o)(\eta_s/a_p) \quad (16)$$

The photoion concentration solute c_s (in gms/cm³) in terms of the final required surface charge density Q_{12} in coulombs/cm² to cancel the voltage difference across the photoion layer is from (3) and (16):

$$c_s = (1/e \eta_o)(m/p) (Q_{12}/a_p) \quad (17)$$

Evaluating c_s in gms/cm³, Q_{12} in coulombs/cm², a_p in m; and $(1/\eta_o e) = 1.04 \times 10^{-5}$ (mol/coulomb)

$$c_s = 1.04 \times 10^{-5} (m/p)(Q_{12}/a_p) \quad (18)$$

6. Initial and Final Capacitance/unit area (mks)

Before the light pulse, in the absence of photoions, the initial capacitance/unit area is C_{11} . Initially the fluid layer capacitance C_p and the glass layer capacitance C_g are in series.

When sufficient ions have migrated to cancel the electric field across the photoion layer, the capacitance/m² of the glass layers C_g equals the final capacitance/m² of the cell C_{12} . The formula relating these initial capacitances is:

$$(1/C_{11}) = (1/C_p) + (1/C_g) \quad (19)$$

Solving (19) for C_{11} :

$$C_{11} = C_g C_p / (C_g + C_p) \quad (20)$$

These capacitances are related to the dielectric constants, and the layer thicknesses as follows:

$$C_{12} = C_g = \epsilon_g \epsilon_o / 2 a_g \quad (21)$$

$$C_p = \epsilon_p \epsilon_o / a_p \quad (22)$$

The change in capacitance/m² is from (20):

$$\Delta C = C_{12} - C_{11} = C_g \{1 - C_p / (C_g + C_p)\} \quad (23)$$

$$\Delta C = C_g \{1/\alpha + (C_p/C_g)\} \quad (24)$$

Let

$$\beta = 1/\alpha + (C_p/C_g) = 1/(1 + \alpha) \quad (25)$$

$$\Delta C = \beta C_{12} = \beta C_g \quad (26)$$

Case I

$$\left. \begin{aligned} C_g &\gg C_p \\ \beta &= 1 \\ \Delta C &= C_g \end{aligned} \right\} \quad (27)$$

Case II

$$\left. \begin{aligned} C_g &= C_p \\ \beta &= 1/2 \\ \Delta C &= (1/2) C_g \end{aligned} \right\} \quad (28)$$

7. Initial and Final Surface Charge Density

The final surface charge density Q_{12} is related to the final capacitance $C_{12} = C_g$ across which the total voltage V appears, as follows:

$$Q_{12} = VC_g \quad (29)$$

The change in surface charge density is, from (26):

$$\Delta Q = V\Delta C = \beta VC_g \quad (30)$$

Initial charge density is from (29) and (30):

$$Q_{11} = Q_{12} - \Delta Q = (1-\beta) VC \quad (31)$$

where

$$\beta = 1/(1 + \alpha) \quad (32)$$

To evaluate α , use (28) and (29):

$$\alpha = (\epsilon_p/\epsilon_g) (2a_g/a_p) \quad (33)$$

8. Initial Voltage Across the Photoion Layer

The voltage V across the cell is the sum of the voltage V_p across the photoion layer, and the voltage V_g across the glass layers:

$$V = V_g + V_p \quad (34)$$

$$(V_p/V) = 1 - (V_g/V) \quad (35)$$

$$V = Q_{11}/C_{11} \quad (36)$$

$$V_g = Q_{11}/C_{12} \quad (37)$$

From (36) and (37):

$$(V_g/V) = (C_{11}/C_{12}) \quad (38)$$

From (35) and (38):

$$(V_p/V) = 1 - (C_{11}/C_{12}) = \Delta C/C_{12} \quad (39)$$

From (26) and (39):

$$V_p = \Delta V \quad (40)$$

9. Photoion Pulse Duration

The time t_o for a photoion to travel a distance a_p in an electric field of intensity $E_p = V_p/a_p$ is:

$$t_o = a_p/u \quad (41)$$

From (1), (40) and (41):

$$t_o = (1/kR)(a_p^2/V) \quad (42)$$

10. Photoion Pulse Current Density

For the voltage across the photoion layer to decrease to zero, a photoion charge per unit area Q_{12} must be deposited on the photoion layer surfaces. The average current density in amps/m² is:

$$i = Q_{12}/t_o = VC_g/t_o \quad (43)$$

The current density versus time is dependent on:

- (a) The time constant of the circuit during the initial charging period including the capacitance C_{11} .
- (b) After the light pulse, on the mobility of the ions produced.

The current density during phase (b) is, from (42) and (43):

$$i = (k\beta) C_g (V/a_p)^2 \quad (44)$$

11. Photoion Mobility

The mobility k depends on the species of ion produced by the ultraviolet light.

For example, if hydroquinone is used, and a free electron is absorbed by the solvent, then the positively charged hydroquinine is a positive ion, and the absorbed electron on the solute is the negative ion.

For example, if a hydrogen ion is produced, then $k \approx 32 \times 10^{-8} \text{ m}^2/\text{volt sec.}$; but if a negative Cl^- ion is produced, then $k \approx 7 \times 10^{-8}$. Since in most cases the

mechanism is presently unknown, the mobility should not be assumed but should be calculated based on an actual observation of the pulse length as well as the measurement of the other factors in the equation. The mobility may be calculated by solving equation (42) for k which then becomes:

$$k = (1/A)(a_p^2/Vt_o) \quad (45)$$

12. Extinction Constant of Photoion Solute

The extinction constant ϵ_s of the photoion solute is defined as the wavelength λ_a at which the photoion solute strongly absorbs uv light, arbitrarily taken as a 1% transmittance for a photoion layer thickness a_p in cm having a photoion solute concentration c_s in gms/cm^2 . The units of ϵ_s are then in cm^2/gm . The mass per unit area of active absorber = M .

$$T = e^{-\epsilon_s c_s a_p} = e^{-\epsilon_s M} \quad (46)$$

$$\ln (1/T) = \epsilon_s c_s a_p = \epsilon_s M \quad (47)$$

for $T = 0.01$

$$\ln 100 = 4.602 = \epsilon_s c_s a_p = \epsilon_s M \quad (48)$$

Experimentally plot T vs. c_s log-linear paper for known values of concentration and transmittance. On the graph find c_s for a cell thickness a_p , for $T = 0.01$, from which:

$$\epsilon_s = 4.602/c_s a_p \approx 46/M \quad (49)$$

13. Proportion p of Photoion Solute Molecules Ionized

The proportion p of the photoion solute molecules ionized is calculated from (3):

$$p = Q_{12}/e \, n_s \quad (50)$$

From (29) and (50):

$$p = VC_g/e \, n_s \quad (51)$$

From (7), (13) and (49):

$$p = VC_g/e \, (n_o/m)(4.6/\epsilon_s) \quad (52)$$

$$p = (1/4.6)(1/e \, n_o) \, \epsilon_s \, m \, C_g \, V \quad (53)$$

$$p = 2.26 \times 10^{-6} \, \epsilon_s \, m \, C_g \, V \quad (54)$$

In (54) C_g is expressed in farads/cm²

14. Differential Electrodynamic Equations of the Photoion Layer

Equations have been set up to represent the conditions illustrated in Figure 5 .

Ultraviolet light initially incident as a photon density N_0 is related to the photon density N at a distance z as follows:

$$N = N_0 e^{-\epsilon_s c_s z} \quad (55)$$

The concentration c_s of the photosensitive molecules is adjusted to absorb 99% of S uv light, whatever the energy.

The photoions initially produced by the uv light pulse constitute an equal positive and negative charge density. The positive and negative charge density depends on the photons of uv light absorbed per unit volume.

$$\rho^+ = \rho^- = -e_u (\partial N / \partial z) \quad (56)$$

From (55):

$$(\partial N / \partial z) = -\epsilon_s c_s N_0 e^{-\epsilon_s c_s z} \quad (57)$$

From (56) and (57):

$$\rho^+ = \rho^- = e \epsilon_s c_s u N_0 e^{-\epsilon_s c_s z} \quad (58)$$

For $z = 0$

$$\rho = \rho_0 = \rho_0^+ = \rho_0^- \quad (59)$$

From (58) and (59)

$$\rho_0 = e u \epsilon_s c_s N_0 \quad (60)$$

The mobility k is:

$$k = u/E \quad (61)$$

The electric field intensity is:

$$E = \partial v / \partial z \quad (62)$$

The current comprises the motion of the positive charge density with the mobility k^+ in one direction, and the motion of the negative charge density in the other direction with the mobility k^- .

The current is also proportional to the electric field intensity:

$$i = (\rho^+ k^+ + \rho^- k^-) (\partial v / \partial z) \quad (63)$$

A charge density in space alters the electric field potential with distance. The space charge equation, known as Poisson's Equation, relates the electric potential versus distance to the space charge.

$$(\partial^2 v / \partial z^2) = -\rho / \epsilon \quad (64)$$

Equation (64) is the one-dimensional form of Poisson's Equation which applies to a thin infinite sheet such as the photoion layer, shown in Figure 6.

The charge density comprises positive and negative charges which co-exist. Initially, when a short, intense uv flash is utilized, an equal number of positive and negative charges exist in a unit volume. If the negative charges are drawn off more quickly, a positive charge density will develop. The net charge density is given by the following formula:

$$\rho = \rho^+ - \rho^-$$

$$\text{Negative current density at } (z + \Delta z) = \rho^-(-u^- + \Delta u^-) \quad (65)$$

$$\text{Negative current density at } z = \rho^- u^- \quad (66)$$

$$\Delta i^- / \Delta z = \Delta(\rho^- u^-) / \Delta z \quad (67)$$

$$= (\rho^- \Delta u^- + u^- \Delta \rho^-) / \Delta z \quad (68)$$

$$= \rho^- (\Delta u^- / \Delta z) + (\Delta z / \Delta t) (\Delta \rho^- / \Delta z) \quad (69)$$

$$= \rho^- (\Delta u^- / \Delta z) + \Delta \rho^- / \Delta t \quad (70)$$

$$= k^- \rho^- (\Delta E / \Delta z) + (\Delta \rho^- / \Delta t) \quad (71)$$

$$i^- = k^- \rho^- E \quad (72)$$

$$\Delta i^- / \Delta z = k^- \rho^- (\Delta E / \Delta z) + k^- E (\Delta \rho^- / \Delta z) \quad (73)$$

Comparing (71) and (73):

Hence:

$$\partial \rho^- / \partial t = k^- E (\partial \rho^- / \partial z) \quad (74)$$

and

$$\partial \rho^+ / \partial t = k^+ E (\partial \rho^+ / \partial z) \quad (75)$$

From (64)

$$\partial \rho / \partial t = \partial \rho^+ / \partial t - \partial \rho^- / \partial t \quad (76)$$

From (64), (65) and (66):

$$\partial \rho / \partial t = [k^+ (\partial \rho^+ / \partial z) - k^- (\partial \rho^- / \partial z)] E \quad (77)$$

From (61), (63) and (64):

$$\partial E / \partial z = -\rho / \epsilon = -(\rho^+ - \rho^-) / \epsilon \quad (78)$$

The initial uv light pulse is absorbed exponentially. Hence the initial charge distribution is exponential with distance into the layer, and equal numbers of positive and negative charges are produced. The exponential constant is the same as ϵ_s the extinction constant.

The boundary conditions are:

$$\begin{cases} \rho^+ = \rho^- = \rho_z = \rho_0 e^{-\epsilon_s c_s z} \\ t = 0 \end{cases} \quad (79)$$

$$\begin{cases} \rho^+ = \rho^- = 0 \\ t = \infty \end{cases} \quad (80)$$

Summarizing:

$$\partial \rho^+ / \partial t = k^+ (\partial \rho^+ / \partial z) E \quad (81)$$

$$\partial \rho^- / \partial t = k^- (\partial \rho^- / \partial z) E \quad (82)$$

$$\rho^+ - \rho^- = \epsilon (\partial E / \partial z) = \epsilon (\partial^2 V / \partial z^2) \quad (83)$$

There are 5 variables ρ^+ , ρ^- , E , z and t , 3 partial differential equations (81), (82) and (83) and 2 boundary conditions (79), (80).

It appears that there are sufficient equations and boundary conditions to arrive at a discreet solution to this problem.

These differential equations establish the nature of the problem and aid in understanding the relationships between the variables.

-27-

These equations will yield a solution for $v = f(z)$ for various values of k^- , k^+ , ϵ_s and n_0 .

Calculations will be carried through using the equations derived in the previous section to serve as a model and standard of comparison for calculations based on experiment. The values chosen for these calculations will be those used experimentally wherever possible.

-28-

Example 1Given: The mobility for the H^+ ion from the Table

$$k = 32 \times 10^{-8} \text{ m}^2/\text{volt-sec.}$$

$$a_p = 135 \text{ mils} = 3.43 \times 10^{-3} \text{ m spacing of fluid}$$

$$a_g = 13 \text{ mils} = 3.3 \times 10^{-4} \text{ m glass}$$

$$\epsilon_g = 5.21 \text{ dielectric constant glass}$$

$$\epsilon_p = 8.68 \text{ dielectric constant fluid}$$

$$V = 10^3 \text{ volts voltage across cell}$$

Find:

$$(1) \beta = 1/(1 + \alpha) \text{ where } \alpha = C_p/C_g$$

$$(2) C_g \text{ in farads/m}^2, \text{ farads/cm}^2 \text{ and pf}$$

$$(3) i \text{ in } \mu \text{ amps/cm}^2$$

Solution

$$\alpha = C_p/C_g = (\epsilon_p/\epsilon_g)(2a_g/a_p) = (8.68/5.21)(2 \times 3.3 \times 10^{-4} / 3.43 \times 10^{-3})$$

$$\alpha = 0.32$$

$$\text{Ans (1) } \beta = 1/(1 + \alpha) = 1/(1 + 0.32) = 0.76$$

$$\begin{aligned} (2) C_g &= \epsilon_0 \epsilon_g / 2a_g = 8.85 \times 10^{-12} \times 5.21 / 2 \times 3.3 \times 10^{-4} \\ &= 7.0 \times 10^{-8} \text{ farads/m}^2 \text{ or } 7.0 \times 10^{-12} \text{ farads/cm}^2 \\ &= 7.0 \text{ pf/cm}^2 \end{aligned}$$

$$(3) \text{ From (44)}$$

$$i = k \epsilon C_g (V/a_p)^2$$

$$i = 32 \times 10^{-8} \times 0.76 \times 7 \times 10^{-8} (10^3 / 3.43 \times 10^{-3})^2$$

$$i = 1.7 \times 10^{-14} (2.92 \times 10^5)^2 = 1.7 \times 10^{-14} \times 8.53 \times 10^{10}$$

$$i = 1.45 \times 10^{-3} \text{ amps/m}^2 \text{ or } 0.145 \mu \text{ amps/cm}^2$$

-29-

Example 2

Given: The mobility for the H^+ from the Table

$$k = 32 \times 10^{-8} \text{ m}^2/\text{volt-sec}$$

$$a_p = 135 \text{ mils} = 3.43 \times 10^{-3} \text{ m spacing of fluids}$$

$$a_g = 13 \text{ mils} = 3.3 \times 10^{-4} \text{ m glass}$$

$$\epsilon_g = 5.21 \text{ dielectric constant glass}$$

$$\epsilon_p = 8.68 \text{ dielectric constant fluid}$$

$$V = 10^3 \text{ volts voltage across cell}$$

$$R = .76$$

Find: Time duration of photoion pulse

Solution:

From (42)

$$t_o = (1/k\epsilon)(a_p^2/V)$$

$$t_o = [1/(32 \times 10^{-8})(0.76)] [(3.43 \times 10^{-3})^2/10^3]$$

$$= (1/24.32 \times 10^{-8})(11.8 \times 10^{-9})$$

$$= 4.9 \times 10^{-2} \text{ seconds or 49 milliseconds}$$

-30-

Example 3Given: The mobility for the H^+ ion from the Table

$$k = 32 \times 10^{-8} \text{ m}^2/\text{volt-sec}$$

$$a_p = 135 \text{ mils} = 3.43 \times 10^{-3} \text{ m spacing of fluid}$$

$$a_g = 13 \text{ mils} = 3.3 \times 10^{-4} \text{ m glass}$$

$$\epsilon_g = 5.21 \text{ dielectric constant glass}$$

$$\epsilon_p = 8.68 \text{ dielectric constant fluid}$$

$$V = 10^3 \text{ volts voltage across cell}$$

Find

$$(a) C_g \text{ in farads/m}^2 \text{ and farads/cm}^2$$

$$(b) Q_{12} \text{ in coulombs/m}^2 \text{ and coulombs/cm}^2$$

Solutions

From Example 1

$$(a) C_g = 7.0 \times 10^{-8} \text{ farads/m}^2$$

(b) From (29)

$$Q_{12} = VC_g$$

$$Q_{12} = 10^3 \times 7.0 \times 10^{-8} = 7.0 \times 10^{-5} \text{ coulombs/m}^2$$

$$\text{or } 7.0 \times 10^{-9} \text{ coulombs/cm}^2$$

-31-

Example 4

Given: A strong uv absorber - 2,2'dihydroxy - 4,4'dimethyl benzophenone (UVINUL 490)

$$C_s = 0.07 \text{ gm/cm}^3$$

$$A_p = 1.3 \times 10^{-3} \text{ cm (light path)}$$

The above C_s and a_p give rise to a transmission of 1% at 390m μ .

Find:

ϵ_s - Extinction coefficient for Uvinul 490 in cm²/gm

Solution: From (17)

$$\log 100/1 = \epsilon_s \times 0.07 \times 1.3 \times 10^{-3}$$

$$2 = \epsilon_s \times 0.07 \times 1.3 \times 10^{-3}$$

$$\epsilon_s = 2 / 1.3 \times 10^{-3} \times 7 \times 10^{-2} = 2 / 9.1 \times 10^{-5}$$

$$= 20 \times 10^4 / 9.1 = 2.2 \times 10^4 = 22,000$$

-32-

Example 5

Using a photoion solute having a molecular weight $m = 100$, and the same value of ϵ_s as in Example 4:

$$a_p = 12 \text{ mils } (3.0 \times 10^{-2} \text{ cm})$$

Find:

- (a) Concentration
- (b) Molecules of photoion solute

Solution:

$$(a) \quad C_s = \log 1/T/a_p \epsilon_s = \frac{\log 100/1}{3.0 \times 10^{-2} \times 2.2 \times 10^4} = 2/6.6 \times 10^2 \\ = 3 \times 10^{-3} \text{ gm/cm}^3$$

(b) The number of molecules/cm² capable of becoming photoions in this example from (13) is:

$$n_s = (n_o/m) C_s a_p =$$

$$n_s = (6 \times 10^{23}/100) 3 \times 10^{-3} \times 3 \times 10^{-2}$$

$$n_s = 6 \times 10^{23} \times 9 \times 10^{-7} = 54 \times 10^{16} \\ = 5.4 \times 10^{15} \text{ molecules/cm}^2$$

-33-

Example 6Given:

The same data as in Examples 4 and 5, and the additional data:

$$\begin{aligned} C_g &= 7.0 \times 10^{-8} \text{ farad/m}^2 \\ &= 7 \times 10^{-12} \text{ farads/cm}^2 \text{ or } 7 \text{ pf/cm}^2 \end{aligned}$$

Find: pSolution

Putting these values in (51):

$$\begin{aligned} p &= VC_g / e \cdot r_s & (85) \\ p &= 10^3 \times 7.0 \times 10^{-12} / 1.6 \times 10^{-19} \times 5.4 \times 10^{15} \\ p &= 7.0 \times 10^{-9} / 8.6 \times 10^{-4} = .81 \times 10^{-5} \\ &= 8.1 \times 10^{-6} = 1/123,000 \end{aligned}$$

Hence only 1 molecule in about 123,000 molecules of the absorbing substance actually absorbs a uv photon, even when a very strong uv absorber is used.

Example 7

We can compute the time required to separate ions from the mobility for Cl^- .

Given

$$k = 6.9 \times 10^{-8} \text{ m}^2/\text{volt-sec.}$$

$$\text{Fluid layer thickness } a_p = 3.43 \times 10^{-3} \text{ m (135 mil)}$$

$$V = 10^3$$

Find: (a) Velocity u

(b) Time for an ion to traverse layer t_o .

Solution:

The velocity is from (61):

$$\begin{aligned} u &= kE = 6.9 \times 10^{-8} \times 10^3 / 3.43 \times 10^{-3} = 2.0 \times 10^{-2} \text{ m/sec} \\ &= 2.0 \text{ cm/sec} \end{aligned}$$

Time for the Cl^- ions to travel a distance a_p and separate is then:

$$t_o = a_p / u = 3.43 \times 10^{-3} / 2.0 \times 10^{-2} = .174 \text{ seconds} = 174 \text{ ms}$$

-35-

Example 8

Given:

The data of Examples 1-7 inclusive and

$$\mu = 1$$

$$t_o = 49 \text{ milliseconds}$$

Find:

(a) Total photons/cm²

(b) Photon intensity

Solution:

From (2):

$$\begin{aligned} (a) \ N &= (p/\mu) n_s = (8.1 \times 10^{-6}/1) \times 5.4 \times 10^{15} \\ &= 4.4 \times 10^{10} \text{ photons/cm}^2 \end{aligned}$$

$$(b) \ \dot{N} = N/t_o = 4.4 \times 10^{10}/49 \times 10^{-3} = 9 \times 10^{11} \text{ photons/cm}^2\text{-sec}$$

-36-

C. Experimental Work

1. Work Program

a) Cell Construction - Cells were constructed so that the motion of ions to the cell walls of suitable dimensions produces a substantial change in the capacitance of the cell. To determine the best cell construction, a study of the capacitance equation enabled us to calculate the cell capacitance and β from the dimensions of the cell.

b) The uv pulse and the gated voltage pulse were displaced on the Memoscope at the same time as the transmitted optical trace.

c) A cell was put into a bridge circuit shown in Figure 8. In the absence of the photoionic effect, the storage scope registers no deflection. If the photoionic effect occurs, then the storage scope will register the differential induced by the uv light pulse. If photoions are produced, they will produce a current pulse in a cell which will constitute this differential.

d) Photosensitive materials described in the literature were tested in a photoion cell.

e) A DC pulse was applied across a cell containing a photoion solution. When the ions separate, a current pulse results which can be measured. The cell is pulsed with uv light and contains only a photosensitive substance in the solvent. In this case there are no dipoles present. The current pulse is observed as a function of the light intensity, pulse duration of

-37-

the light, pulse voltage and duration, DC and/or AC and the concentration and type of photoion solute.

To observe the photoionic effect, various concentrations of promising photoionic solutions were used in the cell. A pulse of uv light was applied onto the cell and with an adjustable delay, a DC voltage pulse across the cell was applied.

Photoionic solutions comprising photoactivators (U.S. Patent No. 2,163,531), photosensitive dyes (U.S. Patent No. 3,112,197) and various photoionic solutes were tested, at first without dipoles; observing the differential current pulse across the bridge circuit.

f) When observing the photoionic effect, using an integrator circuit, the integrated current time or charge vs. time curve will rise to a maximum when the DC voltage pulse is applied across the cell. The ions formed migrate to the surface and coat the inner surfaces of the cell. When the voltage pulse goes to zero, the ions reverse, go back into the solution and neutralize each other. If the process is reversible, the current curve goes negative, and the charge curve on the memoscope decreases to zero. From the data, calculate the electric charge per unit area on the cell wall. From this, along with the cell dimensions and dielectric constant, the change in voltage across the photoion layer can be calculated. If this is of the same order as the initial applied voltage pulse across the layer, the dipole orientation will be substantially modulated.

-38-

g) When a substantial change in voltage across the layer is obtained, then chemically non-reactive dipoles such as lead carbonate crystal or aluminum flake, may be incorporated in the solution without affecting the photoions. A change in orientation and a change in light transmittance should be observable.

h) Use a spectrophotometer to measure uv transmittance vs. wavelength of the photoion solution and determine the extinction constant.

2. Equipment

Figure 7 is a diagram of the experimental setup.

a) The photoion test cell 1 comprises two laminated transparent sheets 2 and 3 with a space between for the layer of photoion solution. The laminated sheets 2 are made of quartz or Corning Corex D glass with a TECOM* transparent conductive lamination and laminated sheets 3 are made of quartz or Corning Corex D glass with a TECOM transparent conductive lamination and laminated sheets 3 are made with two glass sheets with a TECOM transparent conducting lamination.

b) The bridge circuit shown in Figure 8 is used to distinguish between the photoion effect and the ion effect. A uv light pulse and a voltage pulse is applied simultaneously. A trimmer capacitor is included to obtain a null effect in the dark when the circuit is actuated. A differential effect is then

STATINTL

-39-

produced by the uv light. The cells A and B in the bridge circuit are identical and the same voltage pulse is applied to both. However, only cell B receives the uv pulse. The resistors R_1 and R_2 are equal and adjusted so that rise time in cell voltage is small and limits the peak cell charging current. The cell differential current is displayed on a storage scope during the transient period. A DC pulse or a gated AC pulse 10-100kc (0-10KV), is applied across the bridge circuit simultaneously with the ultraviolet pulse.

c) Voltage pulse supply. This combination of units provides a gating pulse of variable duration for a DC voltage and/or an AC voltage of variable frequency 0-200kc. The supply consists of:

One Waveform Generator
40, 4, 0.4, 0.04, 0.004 milliseconds.

One Audio Generator acting
as a frequency generator 0-200kc.

Dipole Power Pack - 0-2000V

A high voltage DC supply (0-20kv) for steady state measurements or when long pulse durations are required. This unit must be operated manually.

d) The ultraviolet pass filter 16 is peaked at 3650Å and cuts off at 3000Å and 4000Å. It is 10cm in diameter, has a peak transmittance of 60% (3650Å), and may be used with any of the uv sources.

e) The quartz lens 21 may be used to obtain a small spot or an image of uv light.

f) Visible light source 10. Visible light is directed from a projection lamp through the photoion cell to a phototube 12 for transmittance measurements. The lamp operates from 115 VAC via a constant voltage transformer 15.

g) The uv filter 17 comprises a coating of UVINUL 490 on a cellulose acetate sheet. Filter 17 absorbs uv light from the uv sources. Only visible light is passed. Its transmittance is less than 1% for wavelengths shorter than 3800Å, and greater than 95% for wavelengths longer than 4200Å.

STATINTL h) The densitometer 13 is a Quantalog matched to the phototube 12, reading in transmittance (100% to 0.01%) and optical density (linear 0 to 4.0).

STATINTL i) The Storage Scope 31 is a 564 MAD which displays two inputs (Y_1 and Y_2 vs. time). The display Y_1 shows the variation in phototube output which corresponds to the transmittance of the photoion cell. The display Y_2 shows the uv pulse duration.

j) The light box, (4' x 4' x 8') which is not shown in Figure 8 surrounds most of the components providing a shield to protect the observer's eyes from the uv source. Half of the front opens on a hinge. In the door in front and on the side are 6" x 6" openings, protected by UVINUL coated filters, to enable viewing of the interior while the uv source is operating.

k) Operation. The photosensitive dipole suspension contains photoions or photodipoles. The window 2 passes ultraviolet light into the photosensitive dipole suspension 1. The ultraviolet light is supplied by an ultraviolet projector 11

-41-

- (i) Constant intensity ultraviolet source
- (ii) Xenon flash
- (iii) Photoflash bulb

Ultraviolet band pass filter 16 transmits ultraviolet light and absorbs visible light. A quartz lens 21 transmits ultraviolet light, and is used to focus an image from plate 20 onto the dipole suspension. The image plate 20 may be removed so that the entire field of the photoion cell is illuminated uniformly. A plate 20 may have a design such as a number of holes or a letter such as "x" punched into a thin metal plate. This design is imaged upon the plane of the suspension. A standard photographic shutter mechanism 19 may be used to control the light. A lamp 10 emits visible light, the intensity of which is maintained constant by a constant voltage transformer 15. Ultraviolet absorption filters 17 and 18 pass visible light.

The effect of the filters is that the photoion cell is illuminated by ultraviolet light only from source 11 and by visible light only from source 10. Only visible light passes through the filter 17. The photocell 12 thus senses a change in the transmission of visible light as influenced by the addition of ultraviolet light. The ultraviolet light itself cannot pass through to the photocell 12 because it is blocked by filter 17.

3) Test Results and Discussion

Various potential photoionic materials suggested in the literature were accumulated and tested as to the extent of their photoionic effect. To date, only three compounds of the many evaluated have given results that merit consideration. These compounds are quinone, diphenylamine and poly-N-vinyl carbazole.

a) Quinone

A solution of quinone in toluol is placed in a cell in a bridge circuit. The cell is illuminated with a steady state moderate intensity uv light using a manually operated light shutter from a type 100-S* source placed 18cm from the cell. The cell was first pulsed without an ultraviolet source with 1700 volts DC for 36 milliseconds. A current pulse having a peak of 1.8 milliamps (0.9 divisions) was observed as a memo-scope trace. (Each division corresponds to a current of 2 milliamps). Then with the ultraviolet source irradiating the cell, the cell was again pulsed with 1700 volts DC for 36 milliseconds. A current pulse having a peak of 4 milliamps (2 divisions) was obtained.

However, it was observed that as the solution aged, a precipitate was formed and the above effect decreased or could not be observed. This deterioration of the solution usually occurs in from 15 to 45 minutes. Although the quinone-toluene system is far from being a practical approach, it does indicate that the photoionic effect does exist.

STATINTL

b) Diphenylamine + chloranil

A solution of diphenylamine and chloranil in benzene was irradiated with ultraviolet light for five minutes but no observable change could be detected on the memoscope. When the diphenylamine-chloranil system was irradiated with a visible light source for 5 minutes, a significant change in capacitance was obtained.

The optimum concentration for this system was found to be 2 grams of diphenylamine and 1 gram of chloranil dissolved in 10 milliliters of benzene.

The cell used in this work was a 3" x 3" VARAD type cell having an active surface area of 25.8 cm^2 . The electrode to electrode distance was 0.197cm and the thickness of the photoionic layer was 0.127cm. The voltage applied across the transparent conductive coatings was 1000 volts DC and the duration of the applied pulse was 4 milliseconds.

The following change in capacitance was observed:

C_g = Capacitance of glass layers = $270_{\mu\text{u}}$ farads

C_{11} = Initial Capacitance of system = $170_{\mu\text{u}}$ farads

C_{12} = Final capacitance of system = $270_{\mu\text{u}}$ farads
(after 5 minutes irradiation
with visible light)

Other concentrations of diphenyl amine and chloranil in benzene and in various other solvents such as chloroform, dioxane, and toluene showed the above effect to a lesser degree.

Examination of the results shown above indicate that irradiation of the photoionic solution formed enough ions to completely shield the electric field across the cell.

c) Poly-N-Vinyl Carbazole

A review of the literature revealed that poly-n-vinyl carbazole (PVK) was potentially a good photoionic material for our system.

After testing many solvents and solvent mixtures, it was found that the best solvent for PVK was a mixture of equal parts by volume of benzene and chloroform.

A solution composed of 0.74 grams of PVK which had been ground in a ball mill, 0.054 grams of phthalic anhydride dissolved in 10 mil of 1:1 CHCl_3 and C_6H_6 was put into a VARAD type cell. The cell had a photoion layer distance (spacer) of 0.11cm. A voltage pulse of 1000 volts DC was applied for 0.4 milliseconds to cell with and without irradiation with ultra-violet light.

After 5 minutes irradiation a capacitance change of 35% was obtained. On irradiating for an additional ten minutes, a total capacitance change of 50% was observed. These orders of magnitude were determined by comparing the traces obtained with the sample with a standard curve which was obtained by connecting capacitors of known value with the bridge circuit.

At this point a series of experiments was made to optimize the PVK system.

Experiment #1

This study was designed to determine the optimum concentration of PVK. A series of solutions with varying accounts of PVK and phthalic anhydride were prepared and tested as previously described. The cell used had a 0.32 cm spacer and an electrode to electrode distance of 0.38cm. The voltage pulse applied to the cell was 1000 volts DC for 0.4 milliseconds.

The data obtained from this work is tabulated below:

Soln. No.	Gms of PVK	Gms of Pthalic Anhydride	millileter 1:1 C_6H_6	Ratio of Capacitance Change*
1	4	0.3	100	1.5
2	3.2	0.3	100	1.8
3	2.7	0.3	100	1.9
4	1.6	0.3	100	1.6
5	4	0.6	100	1.5

*Ratio of Capacitance Change = $\frac{\text{Capacitance} - 5 \text{ minutes UV exposure}}{\text{Capacitance} - \text{Initial}}$

From the above data, it is obvious that the optimum concentration under these test conditions is 0.027gms PVK and 0.003 gms of phthalic anhydride in 100 ml of the $CHCH_5-C_6H_6$ solvent.

-46-

Experiment #2

The effect of phthalic anhydride was investigated. Varying quantities of phthalic anhydride were added to solution of 2.7 grams of PVK in 100 ml of CHCl_3 and C_6H_6 (1:1 by volume). The summary of results of this study is shown below:

Gms Phthalic Anhydride Added	Capacitance (μu farads)				
	Initial	After 5 min of uv	Time after uv Irradiation		
			7 min	30 min	overnight
0	170	310	300	270	---
0.3	170	310	300	300	270
0.6	220	310	310	310	300

This study indicated that phthalic anhydride hinders the rate of the reverse reaction and that an excess of the phthalic anhydride will tend to decrease the total shielding effect.

Experiment #3

It was found that if PVK is dissolved in benzene alone as the solvent, no change is observed between the initial capacitance and the capacitance of the system after 5 and 10 minutes of ultraviolet exposure. Therefore, it is evident that the chloroform plays a role in the formation of ions with ultraviolet irradiation.

-47-

Experiment #4

In this study, the effect of the length of the voltage pulse was examined. Three different pulse lengths were utilized (0.4, 4.0 and 40.0 milliseconds) and it was observed that as the pulse increased, the more completely was the field shielded.

Length of Pulse	Capacitance (μ farads)	
	Initial Capacitance	After 5 minutes uv irradiation
0.4 ms	140	270
4.0 ms	140	280
40 ms	140	300

-48-

Experiment #5

Using our optimum PVK-phthalic anhydride solution, an investigation was made of the effect of voltage on the photoionic effect. The cell used had a photoionic layer distance of 0.13cm and an electrode to electrode distance of 0.19. The voltages applied were DC and the pulse duration was 40 ms.

The data obtained in this study is tabulated below:

Applied Voltage	Ratio of Capacitance Change*
250	1.3
500	1.5
1000	1.8
2000	2.0
*Ratio of Capacitance Change = $\frac{\text{Capacitance} - \text{After 5 min. UV Exposure}}{\text{Capacitance} - \text{Initial}}$	

It is seen from the above data that when the applied voltage pulse is increased, the ratio of capacitance change also increases.

Since the voltage appears to greatly influence the capacitance change of the photoion solution, an attempt was made to determine the effect of the higher voltage on the ultraviolet irradiation time required to obtain a capacitance change that would be sufficient to produce the required shielding phenomenon. In this study, the PVK-phthalic anhydride solution was irradiated with ultraviolet light for a period of 1 minute instead of the previous 5 minute period. The following Table shows the difference in capacitance change observed between a 1000 and 2000 volt DC pulse after 1 minute ultraviolet irradiation.

Applied Voltage	Ratio of Capacitance Change
1000	1.2
2000	1.5

Therefore, higher applied voltages also appear to decrease the time required to obtain a photoionic response.

d) Combined Photoion and Dipole System

The results obtained in the preceding section with PVK and phthalic anhydride describe a system that should be capable of producing a capacitance change that would produce sufficient photoions to effectively shield the electric field used to align a dipole solution.

Therefore, the photoionic material was combined in a common solution with known dipolar systems. It was anticipated that the degree of alignment of the dipole would be substantially different after irradiation of the cell with ultraviolet light.

The first dipolar material tested with PVK was iodo quinine sulfate, which we utilize in our VARAD panels and which has been found to be the most effective dipolar material to date. However, it was found that the iodoquinine sulfate and PVK system, as they presently exist, are not compatible.

To circumvent any incompatibility problems and in order to obtain an immediate indication as to whether or not a photoionic shielding of dipolar alignment could be effected, aluminum powder was tested as the dipolar material. Aluminum had previously shown the ability to align in an electric field and should be

Inert in the PVK system. Incorporation of the aluminum in the PVK solution produced a compatible system, and the following experiments describe the results observed with this solution.

Experiment #1

0.03 grams of ground aluminum power (Alcoa + 1225) was suspended in 10 ml of solution containing 0.27 grams of PVK. This solution was put into a VARAD type cell having an electrode to electrode distance of 0.19cm and a photoion-dipolar layer distance of 0.13cm. The voltage applied across this cell was 2000 volts DC having a pulse length of 0.4 msec.

In this experiment, the testing procedure was to:

1. Record the initial transmittance of the cell;
2. pulse the cell without uv light and record the transmittance of the aligned aluminum dipoles;
3. discontinue the voltage pulse, allow the system to randomize and record new closed transmittance;
4. irradiate with uv light for 5 minutes; and
5. apply pulse and record maximum transmittance to which cell will align.

A typical example of the observed performance of this system is described below:

	% Transmission
Initial Closed Transmittance	5.2
After applying pulse of 2000 volts for 0.4 ms (no uv exposure)	65.0
Discontinue pulse and wait for randomization	15
After 5 minutes uv exposure	15
Applying pulse with uv exposure	23

The results obtained in this experiment indicate that a successful combined photoion-dipolar system has been prepared. The data shows that the photo-induced charge carriers generated do effectively shield the electric field and thus decrease the ability of the aluminum dipoles to align to the degree to which they had been capable before ultraviolet exposure.

Experiment #2

Using the same solution and cell that was employed in the previous experiment, an attempt was made to form an image. In this experiment, a piece of transparent plastic which had been coated with an ultraviolet absorber (UVINUL 490) was used as an ultraviolet filter and fastened to one surface of the cell. The center of the film had a diamond shape cutout. Therefore, the uv light would not irradiate the cell except in the diamond shaped area which had been cut away.

This cell containing PVK and aluminum dipoles was irradiated with uv light for 5 minutes and then had a voltage pulse of 2000 volts applied. The uv light and the pulse were discontinued

-52-

and the UVINUL filter removed. Upon inspection of the cell it was observed that a definite diamond shaped image had been formed in photoionic-dipole solution.

D. CONCLUSIONS

In the short period of investigation into the photoionic dipole effect, we have found two photoion systems which generate sufficient photo-induced charge carriers to effectively shield the electric field across a dipole cell.

In addition, a combined photoion-dipolar system has been developed which has been shown to form a definite image.

The first of the photoion systems that was found effective was diphenylamine-chloranil in benzene. This system was shown to produce a large enough capacitance change on being irradiated with visible light, to shield a dipole aligned field. However, this system was not investigated in any more detail as ions were photo-induced by visible light and would not be of interest to this specific contract.

The PVK-phthalic anhydride in C_6H_6 and $CHCl_3$ system was found to be as effective as the diphenylamine system and the PVK system was photo induced by uv light which is desirable for the research program.

The VARAD cell containing PVK in 1:1 benzene and chloroform showed a capacitance change, after being exposed to uv light, that was equivalent to a total shielding of the field by the photoions produced. This as in the case of diphenylamine-chloranil demonstrated the existence of the photoions.

Part (d) of this section describes the first successful combination of a photoionic material with a dipole. This comprised illuminating a combined PVK-aluminum dipole suspension with uv light and simultaneously subjecting the suspension to 2000 volt DC pulses having a duration of 0.36 milliseconds. Under these

conditions the transmittance changed from 15% to 23%. When the same experiment was repeated with the uv light, the transmittance changed from 5% to 65%.

We were then successful in producing a visible image, by the alignment and disalignment of dipoles under the influence of uv light by combining PVK with an aluminum dipole suspension in a VARAD type cell. This study utilized a uvinol mask with a cutout diamond shape placed in front of the photoionic dipolar cell and illuminated with uv light. The same DC pulses were applied as before. The cell was then observed to show a dark diamond pattern in the center part surrounded by a lighter more transmissive area. This showed that the central area was dis-oriented while the area around the diamond pattern was oriented by the electric field. The feasibility of the photoion-dipolar image forming effect was thus proven.

A theoretical mathematical-physics study has also been presented to consider the interrelationships of the parameters on the basis of known physical laws. These laws have been applied to the present problem and new equations interrelating the parameters have been derived. Now that these new equations are available, they have indicated a procedure for evaluating the parameters which are important to the photoion effect. Moreover, it now becomes possible to compare the experimental results with the order of magnitude of results predicted by theory.

E. FURTHER WORK

1. Preparation of new photoionic solutions.
2. Study of the best photoionic solutions to achieve the greatest voltage shielding and the most rapid response characteristics.
3. Experimental determination of the parameters of the photoion layer.
4. Optimization of the photoion layer.
5. Preparation of other combined photoionic-dipolar system.
6. Determination of the characteristics of the optimum system.

TAB

III PHOTODIPOLES

A. Object

To study the photodipole in an electric field at maximum response frequency for the purpose of orientation modulation by an ultraviolet image.

B. Discussion

One of the approaches was a study in which a uv image modulates visible light, utilizes a fluid layer containing submicron photodipoles in suspension.

The lack of success obtained with the initial experiments prompted the mathematical-physics study presented herein. An important conclusion of the mathematical-physics study is that any dipole may be represented by an RC circuit which has a definite time constant. Utilizing this time constant, there exists an upper limit to the frequency of the applied electric field to which a dipole will respond by orienting itself parallel to the electric field direction. This upper limiting frequency for alignment of the dipoles is herein termed "the maximum response frequency". At a frequency greater than the maximum response frequency, the charging effect at the end of the dipoles on each $\frac{1}{4}$ cycle is small, and the force orienting the dipole is diminished; whereupon the dipole remains randomly oriented.

The mathematical-physics study also reveals that the maximum response frequency varies inversely as the resistivity of the dipole. Since the resistivity is also a function of the illumination of the photodipole, it is now apparent that a means has been discovered to regulate the orientation of a dipole as a function of incident illumination.

The way in which this works is as follows: A photodipole is chosen such that its resistivity varies by at least a factor of 100. The photodipole is then illuminated and its resistivity is decreased to the minimum. At the same time the maximum response frequency is adjusted so that the dipole is aligned at the maximum response frequency. The dipole is thus oriented when and where the illumination is applied. When the illumination is cut off, the dipole resistivity increases and this causes the maximum response frequency to decrease in inverse proportion to the resistivity. Since the maximum response frequency has been set higher than this, the dipoles will now disalign.

The mathematical-physics analysis which follows is based upon an ideal dipole shown in Figure 9, which has the characteristics of two condenser plates connected by the resistor represented by the body of the dipole shown in Figure 10. The dipole is presumed to be made of a material having dielectric constant ϵ and the resistivity ρ , the cross-sectional area of the dipole is A , and the length of the dipole L . The

-3-

applied electric field has the intensity E and the voltage applied across the dipole is then $V = EL$. The corresponding equivalent circuits are shown in Figures 10 and 11.

Figure 10 shows an idealized electrical representation of the dipole. Figure 11 shows the equivalent circuit including a voltage source corresponding to the applied electrical field. Figure 12 shows a curve which corresponds to the exponential charging curve of the condenser in Figure 11.

The general formula for the maximum frequency is derived with relation to the charging curve. An example is given showing a typical range of resistivities and the response frequencies corresponding thereto.

C. Photodipolar Materials

The photodipolar materials are photoconductors. Many photoconductor materials can be grown as crystal whiskers suitable for use as photodipoles, which under controlled conditions can be the general size range required, that is approximately 2000\AA with a length to width ratio of at least 10/1.

Typical materials of this type are zinc oxide, zinc sulfide, selenium, germanium, silicon carbide. Many other photosensitive materials might be suitable for application.

D. Experimental Work

In our initial studies of photodipoles we were able to obtain visible alignment of the zinc oxide dipole suspension. However, although the resistivity of zinc oxide is known to vary substantially with incident uv light, no change in orientation was noted with or without the uv light.

-4-

STATINTL

A small quantity of accicular zinc oxide was obtained having an average particle size of 0.2 microns in the major dimension and having a major to minor ratio of approximately 16 to 1. This accicular zinc oxide sample was produced by a vapor condensation (French) process.

A suspension of the accicular zinc oxide was prepared by grinding 1 part ZnO, 10 parts 20% nitrocellulose solution and 10 parts Celluflex 23 on a ball mill until a smooth paste was formed. The volatile solvents were vacuum evaporated and then resuspended in isopentyl acetate.

This suspension was placed in a three inch standard VARAD cell against a dark background. The suspension appeared faintly milky. The cell was tuned to the optimum frequency for maximum voltage across the cell as previously determined. When the voltage across the cell was increased from zero, the milky appearance became considerably less milky, almost clear. This shows that the elongated particles were aligned.

We attempted to observe a more or less alignment with and without uv light, but there was no apparent difference. However, agglomeration occurred. This was due to the applied voltage (too much or too long), or the uv light or both. The same experiment was repeated with Herapathite. There was no visual difference with the uv light on or off.

It is believed that the residual milkiness observed upon alignment of the present suspension may be due to residual agglomerates that do not align. This can be eliminated by

E. Mathematical-Physics

(a) Symbols

MKS units are used; except as noted.

A	=	Cross section area of dipole	m^2
C	=	Capacitance of dipole - farads	
e	=	2.71	
ϵ	=	Dielectric constant of dipole material	
ϵ_0	=	Dielectric constant of free space	8.854×10^{-12} farads/m
f_m	=	Maximum response frequency,	cps
l	=	Thickness of dipole	
L	=	Length of dipole - m	
ρ	=	Resistivity of dipole - ohm-m	
R	=	Resistance of dipole - ohms	
t_d	=	Time constant of dipole equivalent circuit - sec	
T	=	$1/f_m$ = period of maximum response frequency - sec	

b. Equations

The ideal dipole shown in Figure 9 has a cross sectional area A.

The resistance of the dipole is:

$$R = \rho L/A \quad (1)$$

The capacitance of the dipole is:

$$C = \epsilon \epsilon_0 A/L \quad (2)$$

The time constant t_d of the circuit of Figure 11 is the time for the charge on the ends of the dipole to reach 1/e of maximum:

$$t_d = RC \quad (3)$$

From (1), (2) and (3):

$$t_d = \epsilon_0 \epsilon \rho \quad (4)$$

From Figure 12 it follows that:

$$et_d \cong T/4 = 1/4 f_m \quad (5)$$

From (5)

$$f_m \cong 1/4 et_d \quad (6)$$

The maximum response frequency is from (4) and (6):

$$f_m = 1/4 e \epsilon_0 \epsilon \rho = (1/4 \times 2.71 \times 8.85 \times 10^{-12})(1/\epsilon \rho) \quad (7)$$

$$f_m = (10.4 \times 10^9 / \epsilon \rho) \text{ cps} \quad (8)$$

$$f_m = (10.4 / \epsilon \rho) \text{ kmc} \quad (9)$$

Conversion factor - Resistivity 9 cgs-mks)

100 ohm cm - 1 ohm-m

(c) Example

Given: A photodipole has a resistivity $\rho_1 = 100 \text{ ohm-m}$ (10^4 ohm-cm) in the dark; and a resistivity $\rho_2 = 1 \text{ ohm-m}$ (10^2 ohm-cm) when illuminated with uv light.

The dielectric constant is $\epsilon = 5$.

Find: Maximum response frequency f_m

(a) when illuminated

(b) when dark

Solution:

From (9)

$$(a) \quad f_m \approx 10.4/5 \times 1 = 2 \text{ kmc}$$

$$(b) \quad f_m \approx 10/\epsilon \rho = 10/5 \times 100 = 0.02 \text{ kmc}$$

F. Conclusion

Where the resistivity increases, the response frequency decreases (a longer time is required for the dipole ends A and B to become charged). Above the maximum response frequency the photodipole cannot respond. If the resistivity of the photodipole changes by a factor of 100 (for example from $\rho = 1$ ohm-m to 10^2 ohm-m), then the dipole orientation will be effected by light if 2kmc is applied.

Since the mathematical-physics treatment of the photodipole effect indicate that no response of the material to ultraviolet light could be expected at the frequencies presently available to us, the work on this approach was curtailed until such time as a suitable generator could be purchased or constructed.

G. Further Work Program

1. Prepare various photoconductor materials as crystal whiskers of suitable size to form a photodipole suspension.
2. Construct or purchase equipment that will be capable of producing frequencies in the kilomegacycle range.
3. Employ uv light of appropriate wavelength to cause a suitable charge in resistivity.
4. Study the orientation modulation effect.
5. Derive the operating parameters.

TAB

IV PHOTOCONDUCTIVE ROD MATRIX LAYER

A. Objective

To develop a voltage divider photoconductive layer-dipole combination which demonstrates a high resolution, high contrast, and good quantum efficiency. Figures 13 and 14 show two approaches for achieving this result.

B. Description

Figure 13 shows a matrix comprising photoconductive rods in combination with a dipole layer. The transparent layers 1 and 2 support transparent conductive coatings 3 and 4. The matrix 5 contains the photoconductive rods 6. Transparent insulating layers 7, 8 contain the dipole layer 9. The uv image 10 is focussed by the lens system 11 forming an image 12 within the photoconductive matrix 5. Light source 13 projects a uniform field of visible light 14 on the entire matrix. The orientation of the dipoles 9 is controlled by the change in resistivity produced in the photoconductive rods 6 by the local intensity of the uv image. A filter 15 screens out the uv light from the light 14. The orientation of the dipoles at 9 modulates in the visible light 14 in accordance with the incident uv image 12.

Figure 14 shows a rod matrix in a hexagonal pattern and the geometric relations for a given transmittance.

C. Materials

The following compounds were accumulated as potentially good photoconductors:

Florence Green Seal-8	(ZnO)
Photox-801	(ZnO)
Kadox 15	(ZnO)
Kadox 72	(ZnO)
310 PC	(ZnO)
321 PC	(ZnO)
340 PC	(ZnO)
Titanox Lock	(TiO ₂)
Titanox R-900	(TiO ₂)
Titanox R-47	(TiO ₂)
Titanox AMP	(TiO ₂)
XX-2	(Accicular ZnO)
XX-602	(Accicular ZnO)
Special Sample	(Accicular ZnO)
	French Process

STATINTL

STATINTL

-3-

D. Mathematical-Physics

(a) Symbols

- L = distance between photoconductive rod centers
 D = diameter of the photoconductive rods
 d = distance between transparent conductors
 d₁ = thickness of matrix layer
 d₂ = thickness of transparent insulating layer
 d₃ = thickness of dipole layer
 d₄ = thickness of second insulating transparent layer

(b) Mathematical-Physics

To calculate the (L/D) ratio for 90% transmittance through the matrix, assume:

- (1) the photoconductive rods in the holes are arranged in 60° triangular pattern shown in Figure 14.
- (2) the cross section of the zinc oxide in the holes is 10% of the open area.

Then:

$$\pi D^2 / 4 \times 2 = (0.1) L (\sqrt{3}/4) L \quad (1)$$

This simplifies to:

$$(L/D)^2 = \pi / 0.2 \sqrt{3} \quad (2)$$

From (2):

$$L/D \approx 3 \quad (3)$$

The distance between the transparent conductive layers is:

$$d = d_1 + d_2 + d_3 + d_4 \quad (4)$$

All thicknesses d_1 , d_2 , d_3 and d_4 must be minimized; but, however, a suitable ratio (d_1/d_3) is required to achieve a good switching effect due to the change in resistivity of the photoconductive rods.

E. Experimental Work

1. Work Program

a. The zinc oxide coating may be prepared by ball-milling various proportions of a meltable polymer such as aroclor and ZnO using toluene as a solvent.

Measure the change of resistivity (light vs. dark) with 1:1, 1:2, 1:5 and 1:10 ratios of ZnO/polymer melt solids.

b. Determine the change in resistivity (light vs. dark) of zinc oxide layers of various thicknesses, 1, 2, 3, mils thick. If the change is proportional to the thickness, increase the thickness of the zinc oxide layer until the proportion decreases.

c. The cell is to be fabricated as shown in Figure 13.

i. The zinc oxide layer is coated upon a conductive coated glass sheet. This will admit ultraviolet light to the zinc oxide film.

ii. Place a thin glass sheet over the zinc oxide.

iii. Use an appropriate thickness dipole suspension.

iv. Use another thin glass sheet over the dipole layer. The second thin glass sheet should be coated with a transparent TECOM conductor (our 30-13 formula).

d. Illuminate from the zinc oxide side with uv light and observe the change in dipole transmittance by reflection from the dipole side. The change can be observed in

visible light from the dipole side (See Figure 16).

e. The dipole suspension employed should be a low viscosity suspension in high concentration so that when aligned it will produce a transmittance change from at least 1 to 50%. In this case the aligning field should be a 10 to 20kc AC voltage. The voltage need be only very small, possibly a few hundred volts to achieve the desired result.

f. If the visible change is obtained, then we can instrument the device so as to measure the change by reflection using an appropriate photomultiplier setup. This can be done on the vertical optical bench using a 45° semi-transparent mirror, which will project visible light downward onto the dipole surface and then have this light picked up by the photomultiplier tube above it. The uv light can be applied using a flash tube and a 45° aluminum mirror to the zinc oxide coating side which is on the bottom. (See Figure 16).

-7-

2. Test Results and Discussion

We have observed a resistivity change up to 50,000 to 1 with zinc oxide films in specific cases, but usually 3000 to 1. If we are to use the zinc oxide in a voltage divider device, the dipole layer must be thin in relation to the thickness of the zinc oxide layer. Consequently the dipole layer must be less than $1/3$ the thickness of the zinc oxide layer, preferably about $1/10$. If the zinc oxide layer is of the order of 3 mils, then the dipole layer must be of the order of 1 mil or less. This restriction places rather severe limitations on this method. However, it is certain to work because we know all the components are operable and it is merely a matter of engineering the dimensions and known characteristics of the various layers properly so as to obtain the useful result.

Typical examples of the change of resistivity of (dark vs. ultraviolet light), of the materials listed in Part C of this section, is tabulated below:

-8-

Sample Designation	Resistance (Megohms)		Ratio
	No light	After uv Exposure	
Florence Green Seal -8	1000	0.09	1.1×10^4
Photox 801	1000	10	1.0×10^2
Kadox 15	1000	4	2.5×10^2
Kadox 72	1000	5	2.0×10^2
310 PC	1000	2	5.0×10^2
321 PC	800	3	2.7×10^2
340 PC	800	2.5	3.2×10^2
Titanox Lock	1000	10	1.0×10^2
Titanox R-900	1000	15	0.67×10^2
Titanox R-47	1000	10	1.0×10^2
Titanox A-MP	1000	6	1.6×10^2
XX-2	1000	0.5	2×10^3
XX-602	1000	7.5	1.33×10^2
Special Sample French Process of Accicular ZnO	1000	2.0	5.0×10^2

STATINTL
STATINTL

The results of the above study indicate that
 Florence Green Seal-8 zinc oxide is the most effective photoconductor. Its change of resistivity ratio, upon being irradiated with uv light (1.1×10^4) is almost a magnitude greater than any of the others tested.

-9-

b) Since zinc oxide is a fine powder, it would be difficult to work with unless it were incorporated into a thin film. To this end, materials such as aroclor, pliolite, polystyrene and various other polymers were tested. The material that was found to be excellent for this purpose was a 50% solution of polyvinyl alcohol.

To determine the optimum proportion of Florence Green Seal-8, ZnO and PVA, a series of mixtures were prepared and the results obtained were as follows:

Weight of ZnO	Weight of 50% PVA	Resistance (Megohms)	
		No uv Exposure	After uv Exposure
3.5	3.5	20	.085
2.5	3.5	20	.050
2.1	3.5	20	.085
2.0	3.5	20	.190
1.6	3.5	20	.350
1.2	3.5	20	1.0
0.7	3.5	20	2.0

In the above study all films were maintained at 0.003" thickness and placed between two transparent conductive glass plates. The ultraviolet irradiation used was a type 100-S source held 20cm from the sample for a period of 30 seconds.

From the data it would appear that the optimum paste concentration is 2.5 grams of ZnO to 3.5 grams of PVA

(50% solids) which would give a dry film composition of approximately 60 parts of ZnO to 40 parts of PVA.

c) A study was made to determine the effect of film thickness of the ZnO layer on the change of resistivity (light vs. dark).

Various thicknesses (0.001 to 0.005") of ZnO were prepared and tested in the manner described in the previous experiment. The results are recorded below:

Film Thickness	Resistivity (Megohm)		Ratio
	Dark	After uv Exposure	
.001"	1000	0.9	1.1×10^3
.002"	1000	0.1	1.0×10^4
.003"	1000	0.06	1.7×10^4
.004"	1000	0.08	1.25×10^4
.005"	1000	0.4	2.5×10^3

This study shows that the optimum thickness for the ZnO layer is 0.003" (0.0076cm). At film thicknesses greater than .003" the ultraviolet light does not pass through the full film thickness and thus the resistance ratio starts to decrease.

Therefore, in accordance with the mathematical-physics study described in part D of this section, a maximum dipole layer of 0.001" is required.

d) The above study indicates that the use of a .003" ZnO layer used in conjunction with 0.001" thick dipole cell

would force such severe limitations on the system as to make it impractical. Therefore, a new approach, the photoconductive rod matrix, was initiated.

The rod matrix approach affords much more latitude in the ZnO layer thickness. The uv source can irradiate the long thin ZnO rod along its length which, in effect, simulates a thicker film layer.

To test this approach, a rod matrix cell was prepared containing all the elements described in Figures 13 and 14.

A sheet of plexiglass 2.0mm thick was drilled with holes 0.5mm diameter spaced 2.0mm apart and connected with thin conductive strips on one side to a source of potential. A VARAD type cell having only one electrode was placed with its plain glass panel close up against one end of the photoconductive rod plate. The VARAD type cell contained an herapathite suspension having a q_{rz} of approximately 10. A voltage of 1.5 kilovolts was placed across the transparent conductive coating on the front side of the VARAD type cell and the other side of the circuit was connected to the photoconductive rods.

The zinc oxide photoconductive rods were irradiated over a portion of the rods to decrease their resistivity which decreased from 10^8 ohms to 10^5 ohms. The uv light employed was a B-100 Spectroline lamp located 10cm from the photoconductive rods. Upon adjusting the frequency and voltage, the illuminated rods clearly caused a transparent area to form in the VARAD suspension. The rods which had not been illuminated did not cause the corresponding area of the VARAD suspension to open.

-12-

A clearly outlined pattern of dots was formed that was visible from the front surface of the VARAD suspension. The VARAD cell appeared dark except in those areas which opened up and where the light reflected from the ends of the photoconductive rods to produce a visible pattern.

F. CONCLUSIONS

STATINTL In this section of the report it has been determined that the most effective photoconductor was Florence Green Seal-8 and that the optimum paste composition was 60 parts of ZnO to 40 parts of PVA.

The optimum ZnO film thickness was found to be 0.003". Since this was thought to place severe restrictions on the system, our attention was turned to the rod matrix effect.

Our experimental results with the photoconductive rod matrix effect has brought this system to the point where feasibility has been shown.

G. FURTHER WORK PROGRAM

1. Prepare a photoconductive matrix structure comprising zinc oxide-polymer rods similar to that shown in Figure 13.
2. Assemble the photoconductive matrix with a dipole layer in the device shown in Figure 13.
3. Determine the relationship between the thickness d , d_1 , d_2 , d_3 , d_4 for the optimum cell. The overall thickness d must be kept at a minimum to achieve maximum resolution.
4. Determine the relationship between the dimensions of the various elements of the structure and the operating characteristics of the structure:
 - (a) Image resolution
 - (b) Change in optical density of the dipolar medium induced by the intensity of uv light focussed upon the photoconductive matrix to form an image.
5. Work on the resistivity of ZnO layer should be repeated with the rod matrix layer so as to make sure that we have an optimum result. Repeat this experiment with various proportions of PVA or other polymers. Measure the resistivity with about 1/1, 1/2, 1/5 and 1/10 concentration of ZnO/PVA solids. Take measurement random and oriented.
6. ZnO incorporated into new polymers, combinations of polymers and/or dopants should be investigated.

TAB

V ORIENTED DIPOLE PHOTOCONDUCTIVE LAYER

A. Description

Figure 15 shows a photoconductive layer structure comprising accicular zinc oxide crystals permanently oriented normal to the plane of the matrix layer. The accicular crystals are of micron or submicron dimensions. A small proportion of an ionic conductor (such as lithium chloride) dissolved in the transparent matrix 21, bridges the photoconductive crystals 20.

The oriented crystal photoconductive layer shown in Figure 15 is a more advanced and sophisticated concept than the photoconductive rod matrix layer shown in Figure 13. This layer structure is more readily fabricated than the photoconductive rod structure.

The resolution of this system, utilizing thin insulating layers between the oriented photoconductive matrix and a thin dipole layer in contact therewith, should be between a 10 and 100 lines per millimeter.

B. DISCUSSION

The oriented dipole photoconductive layer approach is a sophisticated version of the conduction rod matrix system which is covered in the previous section.

We have shown the feasibility of using conductive rods to form an image. The orientation of a conductive dipole in a polymer melt would give, in effect, a simple sophisticated method in which to form a rod matrix. This dipole layer would contain many times the number of photoconductive rods than it would be possible to pack in any other type of matrix.

Although no program has been initiated on this approach, the probability of obtaining a successful system is excellent.

Section IV of this report indicates that two of the requirements for this approach are available: (1) the photoconductive rod matrix does form an image; (2) photoconductive zinc oxides capable of alignment (accicular) has been shown to possess a relatively high resistance charge ratio (xx-2 and the French Process accicular zinc oxide).

C. Further Work Program

Prepare and study a layer comprising an oriented accicular photoconductive crystal 20 in a matrix 21, as shown in Figure 15.

1. In various thicknesses.
2. With various compositions.
3. With various ratios of aligned photoconductive crystals to polymer matrix.
4. Various proportions and types of dopants in the matrix.

TAB

VI QUESTIONS AND ANSWERS

Q-1. If a certain level of U-V radiation is required to ionize the molecules, then a higher level must be transmitted through the film because certain losses are incurred at the interfaces of the screen, and due to internal reflections before the radiation reaches the dipolar layer. What is the actual quantum efficiency?

A-1. The ultraviolet pulse on the dipole cell layer is absorbed exponentially, as shown in Figure 4. The photoions initially have an exponential distribution in space.

For an efficient photoion layer, the layer thickness and a concentration of photoions is established such that at least 99% but not more than 99.9% is absorbed in the layer. We can assure this by providing suitable photoion layer thickness and concentration of photoion particles. (See Section II-B, p. 21). The reflection loss will occur only at the first surface and will, therefore, be of the order of 4%. The indices of refraction of all other surfaces are approximately matched. No consideration need be given to the exit surface reflection loss since the ultraviolet light will be more or less totally absorbed within the photo layer. We can, therefore, state that 96% of the ultraviolet light will be available for use within the photoion layer.

The actual quantum efficiency is another matter. In certain cases the quantum efficiency of the photoion substance is known from the literature. The quantum efficiency and its

-2-

relation to other parameters of the photoion layer is discussed in Section 11-B, p. 13.

Actually the quantum efficiency could exceed 1. This is due to the possibility that a sufficiently strong electric field will cause a cascading effect once ions are produced by the ultraviolet photon. The cascading effect is produced by energy provided by the field which causes pairs of ions to collide with solute molecules, producing additional pairs of ions therefrom in a chain reaction. The extent to which the cascading effect occurs depends on the strength of the applied electric field which is a parameter of the multiplication factor. This complicated effect should be investigated experimentally.

Below a critical applied electric field intensity, the actual quantum efficiency without the cascading effect, varies with the nature of the photoionic substance employed, and must be determined experimentally.

Q-2. What is the attenuation of the original imagery by the screen?

A-2. The original imagery which is born by ultraviolet light is substantially totally absorbed by the screen. Very little, if any, ultraviolet light need pass through the screen.

Q-3. What is the selectivity of the Ultraviolet illumination?

A-3. The selectivity of the ultraviolet illumination depends upon the absorption curve of the photoionic solute. These absorption curves vary with the nature of the photoionic solute

-3-

employed and each photoionic solute will have its own specific characteristic which must be determined experimentally.

Q-4. Will the U-V illumination control the screen to the same degree as it is transmitted by the original; i.e., is the system linear?

A-4. Typical curves transmittance vs. time for various applied electric field intensities for a suspension of herapathite dipoles is shown in Figure 17. The formula for this curve has been previously derived and given elsewhere³¹. The curves represent a double exponential variation of transmittance with time. From the curves it is evident that a great change in transmittance is produced by a relatively small change in voltage.

Figure 18 shows that the change in optical density is approximately linear with a change in electric field intensity.

Q-5. Will the projected image be as sharp as one on a conventional rear projection screen?

A-5. Since the order of magnitude and the thickness of the photoion layer is the same as the order of magnitude of thickness of the rear projection screen; that is, from 5 to 30 mils in thickness, the projected image should be as sharp as that of a conventional rear projection screen.

-4-

Q-6. The ionized material will de-ionize with time. The de-ionization will be rapid at first since the voltage gradient will decrease as the ions move away from the wall surfaces toward each other, recombining as they do.

A-6. The ionized material will de-ionize with time. The de-ionization will be rapid at first since the voltage gradient will decrease as the ions move away from the wall surfaces toward each other, recombining as they do.

With regard to the variation of ionizing characteristics with age and extended use, this will depend upon the photochemical system chosen. The photo-chemical system should be chosen for complete reversibility. Certain photochemical systems are known which contain reversible ions³². The reversible ions are caused by change of valence or charge per ion. Examples of these systems are the ferric-ferrous chloride systems Fe^{+++} , Fe^{++} as a photoion. Because FeCl_3 solution is very sharp yellow and is light reactive, it is likely to be a good reversible source of photoions. Other ionic systems known to be reversible are:

Ti^{+++} , Ti^{++} ; Cr^{+++} , Cr^{++} , Ce^{++++} , Ce^{+++} , Co^{+++} , Co^{++}

The variation of ionizing characteristics with each and extended use will depend upon the choice of system employed. As given above, certain systems are known to be indefinitely reversible. They are also known to be light reactive.

It is proposed to study these systems most intensively. Various other known photoionic materials have usually been used in photo reproduction processes where the materials are used but once, and where the matter of reversibility is unexplored, since there has been no need for repeated use. The many such materials which our search has uncovered⁹⁻²⁹ must be systematically studied for their utility for use with this system.

Q-7. Will the internal reflection of the U-V, due to the interfaces of the screen affect the presentation?

A-7. It can be definitely stated that internal reflection of the ultraviolet due to the interfaces of the screen will not affect the presentation as previously shown. The only reflection is the single external first reflection. The ultraviolet light is transmitted through the glass, the transparent conductive layer and the photoion layer without internal reflection. The photoion effect is obtained by the absorption of the ultraviolet light. Consequently internal reflection is not expected to be a problem and have no effect upon the presentation.

-6-

Q-8. Since the screen is a fluid, there could be thermal gradients due to uneven heating; will this affect the presentation?

A-8 With regard to thermal gradients due to uneven heating, let us assume that a liquid flow does occur due to such heating. Such flow would be relatively slow and would in any case require much longer than the time constants of the photoions or the dipoles. Hence thermal gradients will produce no effect provided, however, that the temperature of the fluid is not sufficient to cause the formation of bubbles, or the deterioration of the components of the solution.

There will be no effect upon the presentation due to thermal gradients, when the intensity of the light being transmitted is below the temperature at which coagulation, deterioration or vaporization of the fluid is effected.

Q-9. How will the electric field be controlled?

A-9. The electric field will be a uniform electric field which is applied as a DC pulse, or as an AC field operating at a DC level in the form of a pulse modulation of a train of waves.

Q-10. What will the time required for the ions to recombine when the field is released?

A-10. When the field is released the reverse field of the same magnitude will be established within the solution. The recombination time will, therefore, be of the same order of magnitude as the original separation time after the formation of

-7-

the ions by the ultraviolet light. This is of the order of a few milliseconds according to present observations and calculations. (Figure 17). When the screen is fully open, its transmittance is expected to be of the order of 60-70%. This is fairly close to that of the conventional screen. However, in a light amplifier or light modulator portions of the screen must absorb light rather than transmit light to create a visible image. For example, the screen transmittance will vary from 1% to 70%. (See Figure 17, according to the locally applied field intensity).

Q-11. Is the energy level that is required to pass through the film less than that presently transmitted through the film in conventional rear projection viewers?

A-11. It is expected that the energy level which passes through the photoion layer will be of the same order of magnitude as that presently transmitted through the film in conventional rear projection views.

Q-12. To what degree will there be migrations of the ions over the surface of the screen - causing blurring of the image -- after the screen has been illuminated.

A-12. It is expected that the migration of the ions over the surface of the screen sideways will be of the same order of magnitude as the thickness of the photoion layer. Therefore, the size of the image projected on the photoion screen is

related to the thickness of the screen in the ratio of the number of lines of resolution which is required. For example, if a 1,000 line resolution is required and the photoion dipole layer thickness is of the order of 0.1 mm (4 mils) then the size of the screen must be 100 mm (4 in.).

Q-13. How long can an image be held without any significant loss of quality?

A-13. The migration of ions sideways will depend upon the side voltage gradients. It is expected that image quality will gradually deteriorate due to voltage gradients being set up in the plane of the image by the concentration of ions in dark areas and the corresponding lack of ions in the lighter areas. Another method is to use a large area compared to thickness in which case the image could be held indefinitely. The deterioration of the image can be calculated from the known ion concentrations required for adjacent black and white areas and the known mobilities of the ions involved. The image deterioration will be determined experimentally in Phase II.

Methods of retaining full sharpness of the image are as follows:

(1) Utilization of cellular construction of the screen in which the individual cells are of the same order of dimension as photoion film thickness.

(2) The area of the screen is made large relative to the thickness.

(3) The visible image is electrically dispersed by orientation of the dipoles during an ultraviolet image blackout. Thereafter it is reformed again and allowed to remain so long as image quality is satisfactory. Thereafter it is wiped out and the cycle repeated. This may be done rapidly enough to form a continuously projected image.

Q-14. Does the energy from the auxiliary illumination affect the dipole suspension? If so, how and to what degree does it affect the output presentation?

A-14. The energy from the auxiliary illumination will affect the dipole suspension only if the dipole suspension is temperature sensitive. In the case of the herapathite suspension the upper limit is about 75°C. In the case of metal dipolar suspensions the upper limit is the boiling point of the fluid employed. If the screen is operated below these temperatures, there should be no effect upon the upper presentation.

Q-15. What will be the quality of the output presentation with respect to:

- (a) Modulation Transfer Function.
- (b) Density Range
- (c) Density discrimination

A-15 (a) In the photoion effect there is a change in electric field intensity which is linear with the intensity and time of the incident ultraviolet light. (See Section II, Equation 10) The electric field gradient across the photoion-dipole layer is linear with a change in the energy of the incident ultraviolet light pulse. However, the corresponding change in dipole transmittance is a complicated double exponential function of the change in electric field intensity, while the change in optical density is an approximately linear function. Therefore, we can conclude that the modulation transfer function with respect to the density optical of the visible image produced will be linear with respect to the intensity of the uv light image.

(b) The fixed range will depend upon the electro-dichroic ratio. With the herapathite dipoles an electro-dichroic ratio or density ratio of 10 or 15 to 1 may be obtained. With ideal metal dipoles the predicted density ratios can be up to a maximum ideal ratio of 150 to 1, but probably more practically would be in the range of 20 to 30.

(c) The density discrimination will be a function of the actual parameters of the modulation transfer function given above. The modulation transfer function is actually known insofar as its relation to the electric field intensity is concerned.

The electric field intensity is also known to be related to the intensity of the incident ultraviolet light. While these two functions are known and both of them have actually been determined experimentally, the combination of the two have not been experimentally observed. This work will be performed in the proposed continuation of Phase I.

TAB

VIII -

REFERENCES

1. Polymeres Semi-Conducteurs by F.X. de Charentenay, P. Castel et Ph. Teyssie. Revue de L'Institut Francais Du Petrole et Annales des Combustibles Liquides, Vol. XVIII, no. 9, September 1963, pp. 1265-1266.
2. Limitations and Possibilities for Improvement of Photo-voltaic Solar Energy Converters, M. Wolf, IRE, August 19, 1959.
3. Experiments on the Interface between Germanium and an Electrolyte, W. H. Brattain and C.G.B. Garrett, Bell System Technical Journal, Jan. 1955, p.129
4. The Role of Light in Photosynthesis, Daniel I. Arnon, Reprinted from Scientific American, November 1960.
5. The Path of Carbon in Photosynthesis, J. A. Bassham, Reprinted from Scientific America, June, 1962.
6. The Continuous Absorption Spectrum of Hydrogen Iodide, C.F. Goodeve and A.W.C. Taylor, The Sir William Ramsay Laboratories of Inorganic and Physical Chemistry, University College, London.
7. The Absorption Spectrum and Photochemical Decomposition of Hydriodic Acid, G. K. Rollefson and J.E. Booher, Journal of the American Chemical Society, Vol. 53 No. 5 May, 1931, p. 1728.
8. Crystal Structure and Photoconductivity of Cesium Plumbahalides, C.K. Moller, Chemical Laboratory, Royal Veterinary and Agricultural College, Copenhagen.
9. On the Sensitization of the Anthracene by Organic Dyes, B. J. Mulder and J. De Jonge, Koninkl Nederl Akademie Van Wetenschappen - Amsterdam - Reprinted from Proceedings, Series B, 66, No. 5, 1963.
10. Optical and Electrical Properties of ZnO Crystals, Hideo Watanabe, Masanobu Wada, Department of Electronic Engineering, Japanese Journal of Applied Physics, Vol. 3 No. 10, October 1964.
11. Dye Sensitized Photo-response in Organic Semiconductors, V. Mylnikov and A. Terenin, Physics Dept. Leningrad University USSR.
12. On Photoelectric Effects in Polymers and Their Sensitization by Dopants, Helmut Hoegl, Battelle Memorial Institute, Carouge, Geneva, Switzerland, 1964.

REFERENCES (Cont.)

13. U.S. Patent No. 3,163,531, Photoconductive Layers for Photographic Purposes, Heinz Schlesinger.
14. U.S. Patent No. 3,112,197, Electrophotographic Member, Wilhelm Neugebauer, et al.
15. U.S. Patent No. 3,037,861, Electrophotographic Reproduction Material, Hoegl.
16. U.S. Patent No. 3,041,165, Electrophotographic Material, Oskar Sus, et al.
17. U.S. Patent No. 3,072,479, Electrophotographic Plates Comprising Solid Solutions of Oxazolones, Gunther Bethe.
18. U.S. Patent No. 3,112,197, Electrophotographic Member, Wilhelm Neugebauer, et al.
19. U.S. Patent No. 3,113,022, Electrophotographic Process, Paul Maria Cassiers, et al.
20. U.S. Patent No. 3,131,060, Electrophotographic Material, Paul Maria Cassiers, et al.
21. U.S. Patent No. 3,139,946, Electrophotographic Material and Process, Hans Schlesinger.
22. U.S. Patent No. 3,140,946, Electrographic Material, Paul Maria Cassiers
23. U.S. Patent No. 3,161,505, Material for Electrophotographic Purposes, Martha Tomanek
24. U.S. Patent No. 3,114,633, Material for Electrophotographic and Electroradiographic Purposes, Hans Schlesinger
25. U.S. Patent No. 3,155,503, Electrophotographic Material, Paul Maria Cassiers
26. U.S. Patent No. 3,163,532, Material for Electrophotographic Purposes, Hans Schlesinger
27. French Patent No. 1.254,348
28. German Patent No. 1110007

REFERENCES (cont.)

29. "Development of Systems for Automatic Reversible Control of Intensity of Visible Radiation Through Transparent Materials" AD 261 272
30. Source: From Mr. Hank Pence of the St. Joseph Lead Company, as a small scale laboratory sample via Dr. Thomas J. Kucera of American Photocopy & Equipment Company.
31. Brooks Air Force Base Proposal No. 64-1101, page 83, formula 92.
32. "Ions in Solution" by Gurney - p. 135; pp. 97-98; pp.110-117

STATINTL

TAB

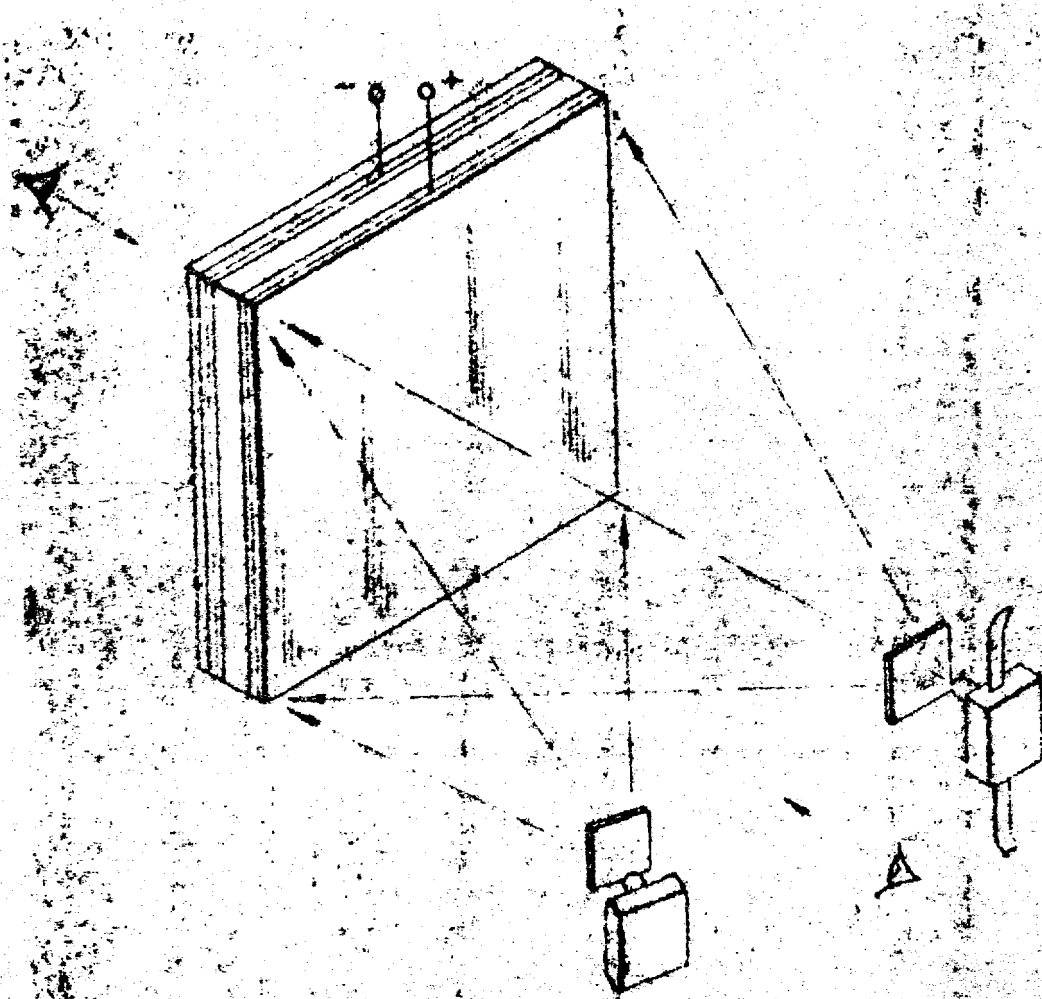


FIGURE 1

shows a light amplifier, whereby an ultraviolet image is utilized to modulate visible light amplifying a photonic dipole device.

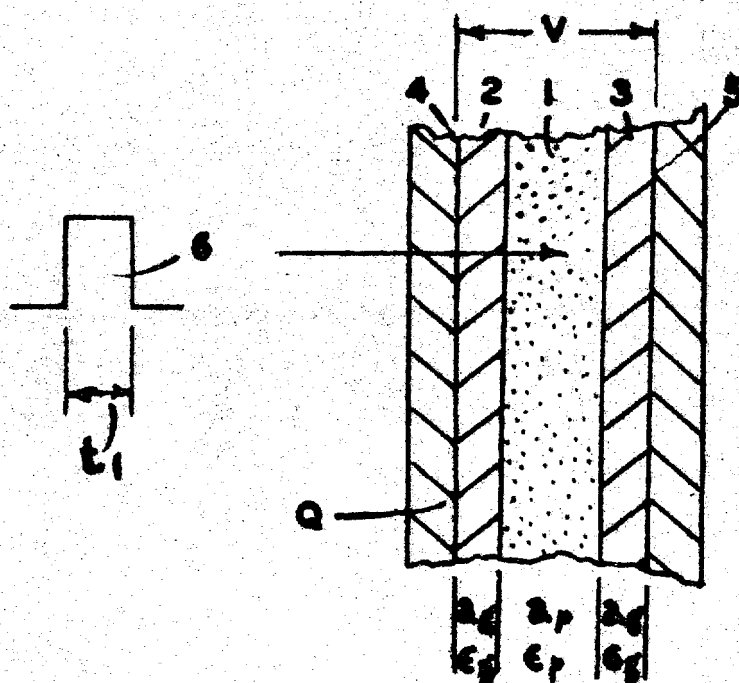


FIGURE 2

shows a cross section of a photolaminate between laminated glass sheets, each laminate containing a transparent conducting layer, and an incident uv light pulse.

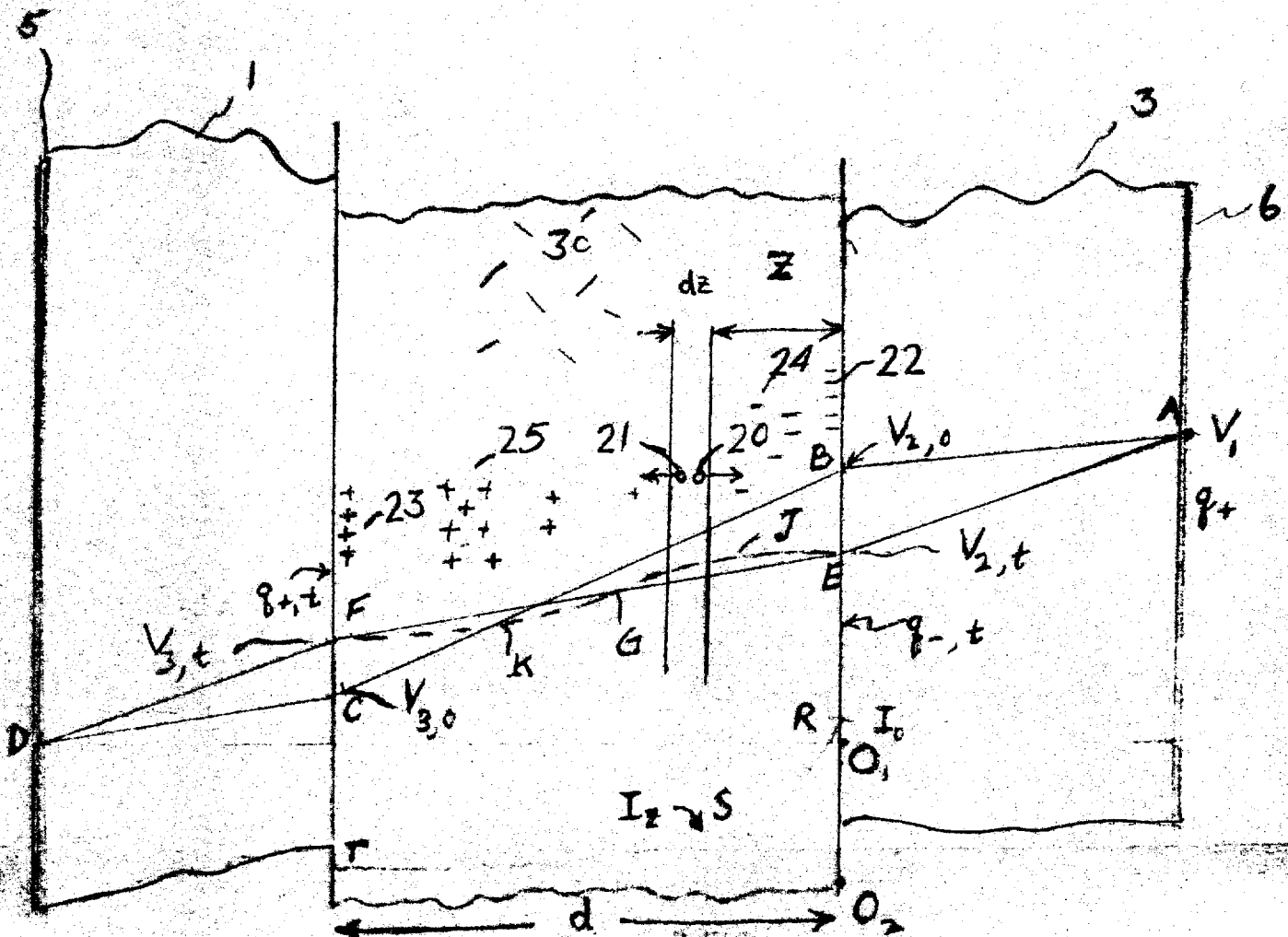


FIGURE 3

shows the potential distribution across the space between the transparent electrodes of Figure 2.

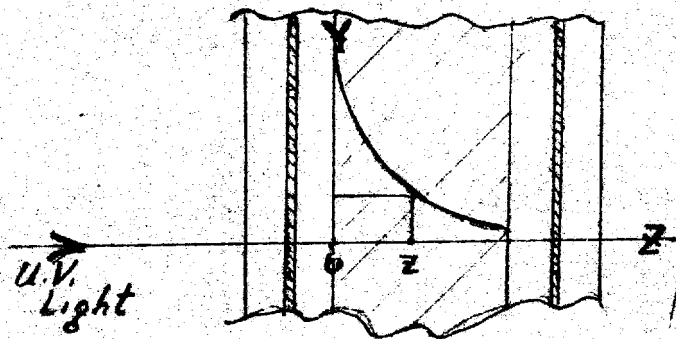


FIGURE 4

shows the ultraviolet pulse on a photoion cell layer absorbed exponentially. The photoions initially have an exponential distribution in space.

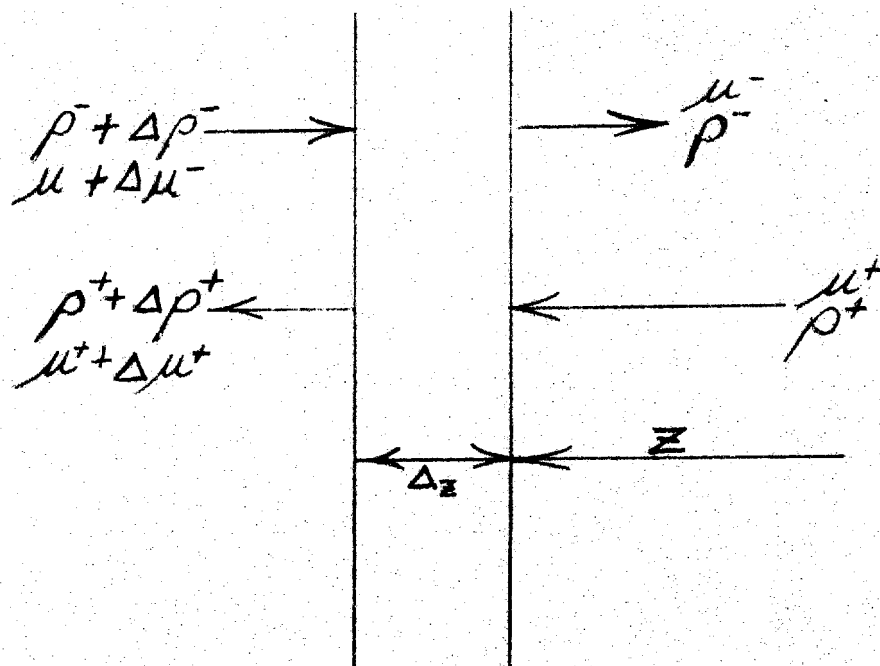


FIGURE 5

shows dynamic conditions within a photoion layer. The charge density and velocity of positive and negative ions are shown entering and leaving a photoion layer of thickness Δz , at a distance z from one face of the photoion layer

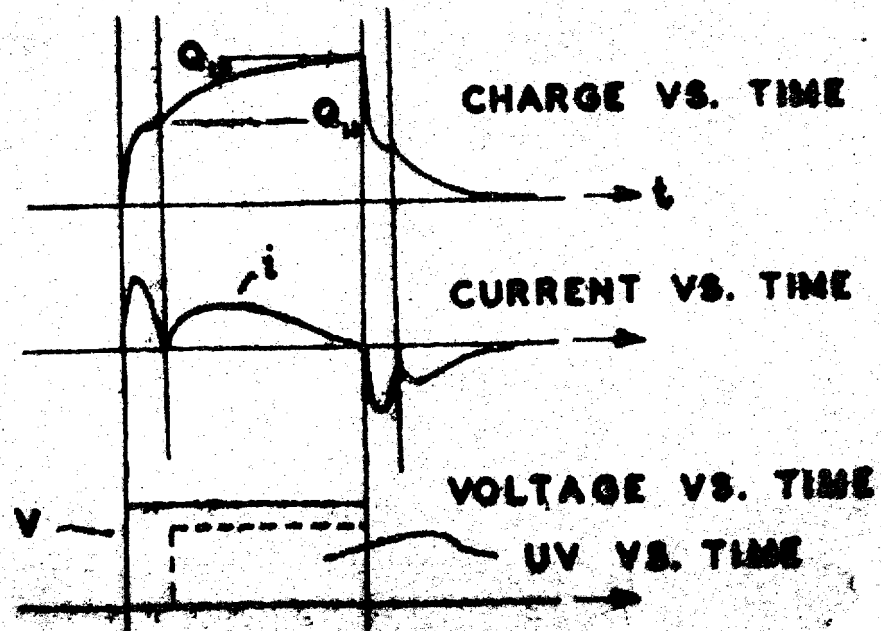


FIGURE 6

shows the surface electric charge density and the surface current density vs. time in a photoion cell subjected to a square voltage pulse and a square uv light pulse.

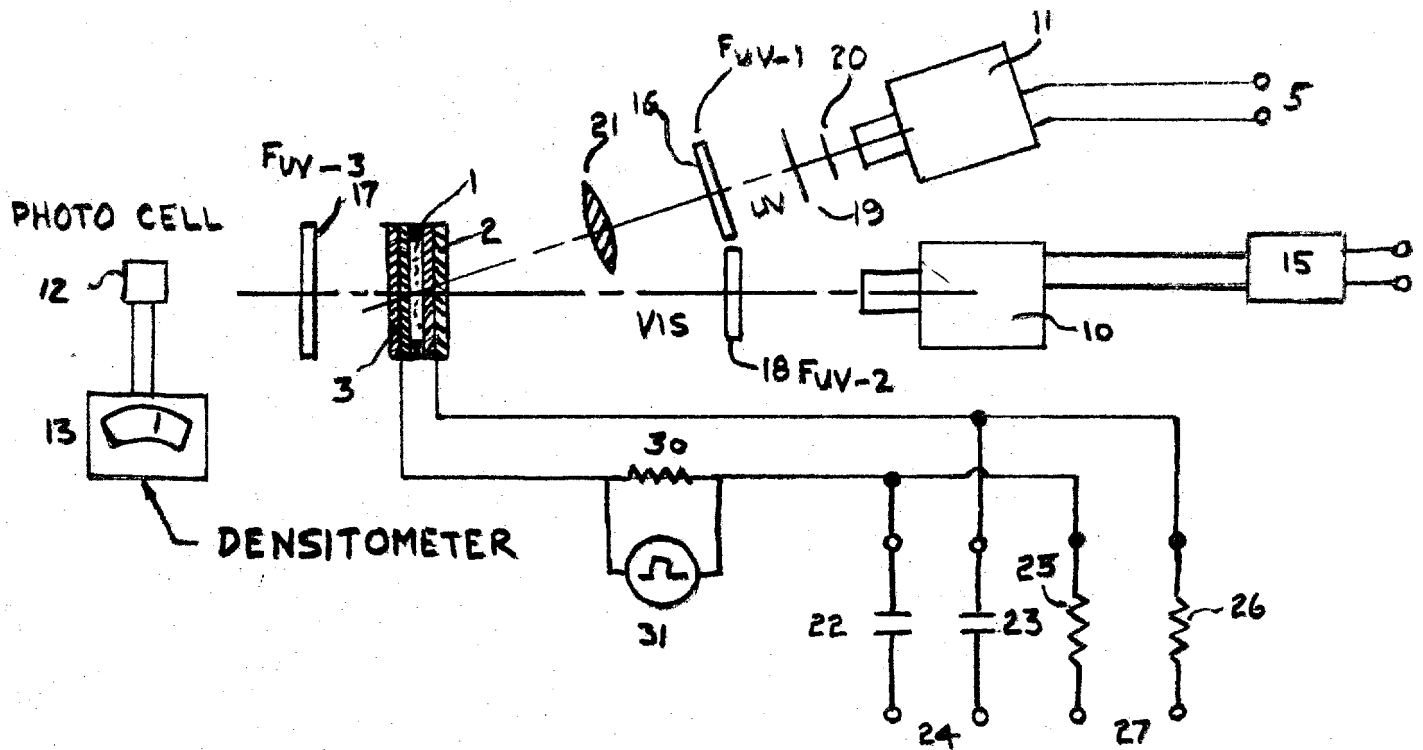


FIGURE 7

shows the experimental setup for the study of the photoion effect.

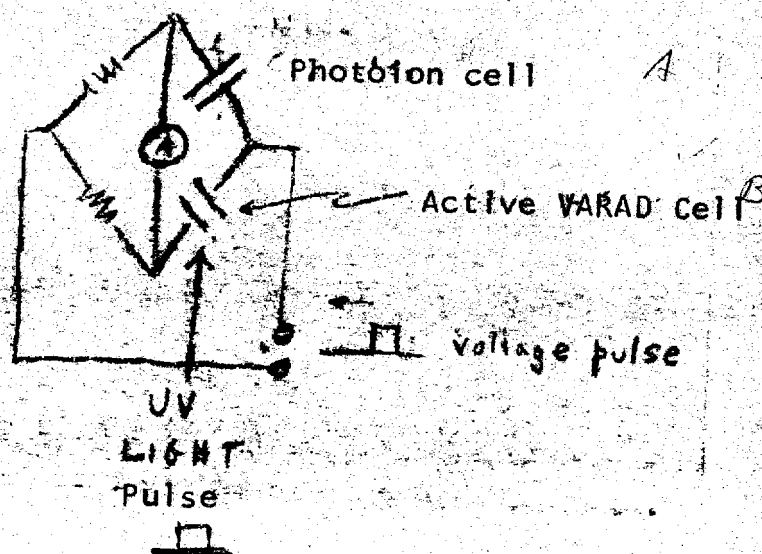


FIGURE 8

shows bridge circuit in which two identical photon cells are placed, only one of which is exposed to the uv light pulse, to distinguish the photon effect from just an ion effect.

shows an ideal dipole rod.

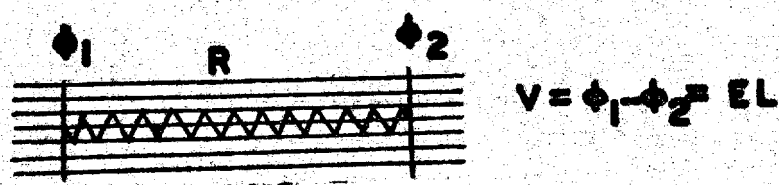


FIGURE 10

shows equivalent dipole.

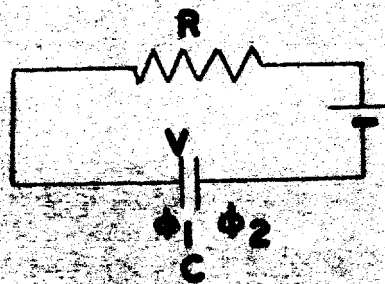


FIGURE 11

shows equivalent circuit of dipole in an electric field.

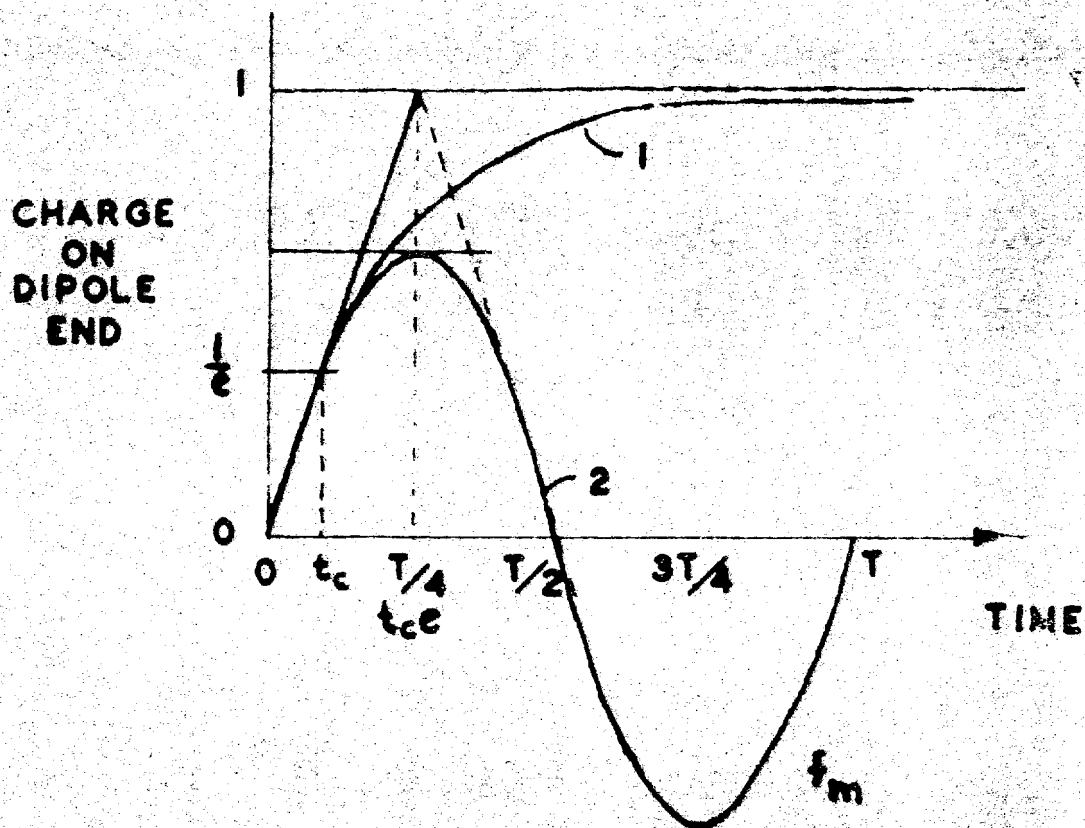


FIGURE 12

SHOWING CHARGE RISE TIME CURVE, 1, AND SINE WAVE, 2, OF APPLIED A.C. FIELD CORRESPONDING TO MAXIMUM FREQUENCY, f_m

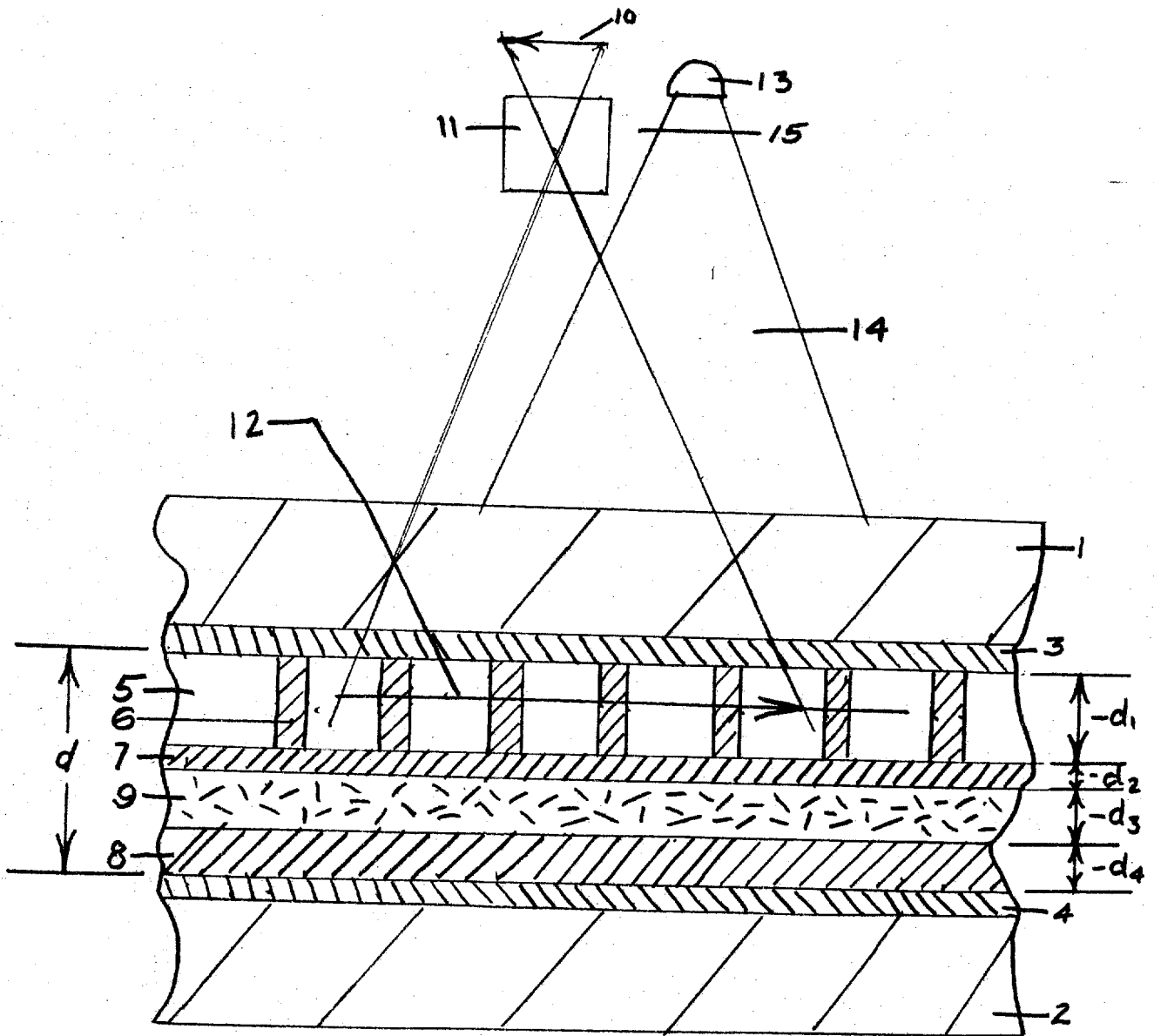


FIGURE 13

shows a photoconductive rod matrix and dipole layer utilized as a light amplifier which is actuated by ultraviolet light.

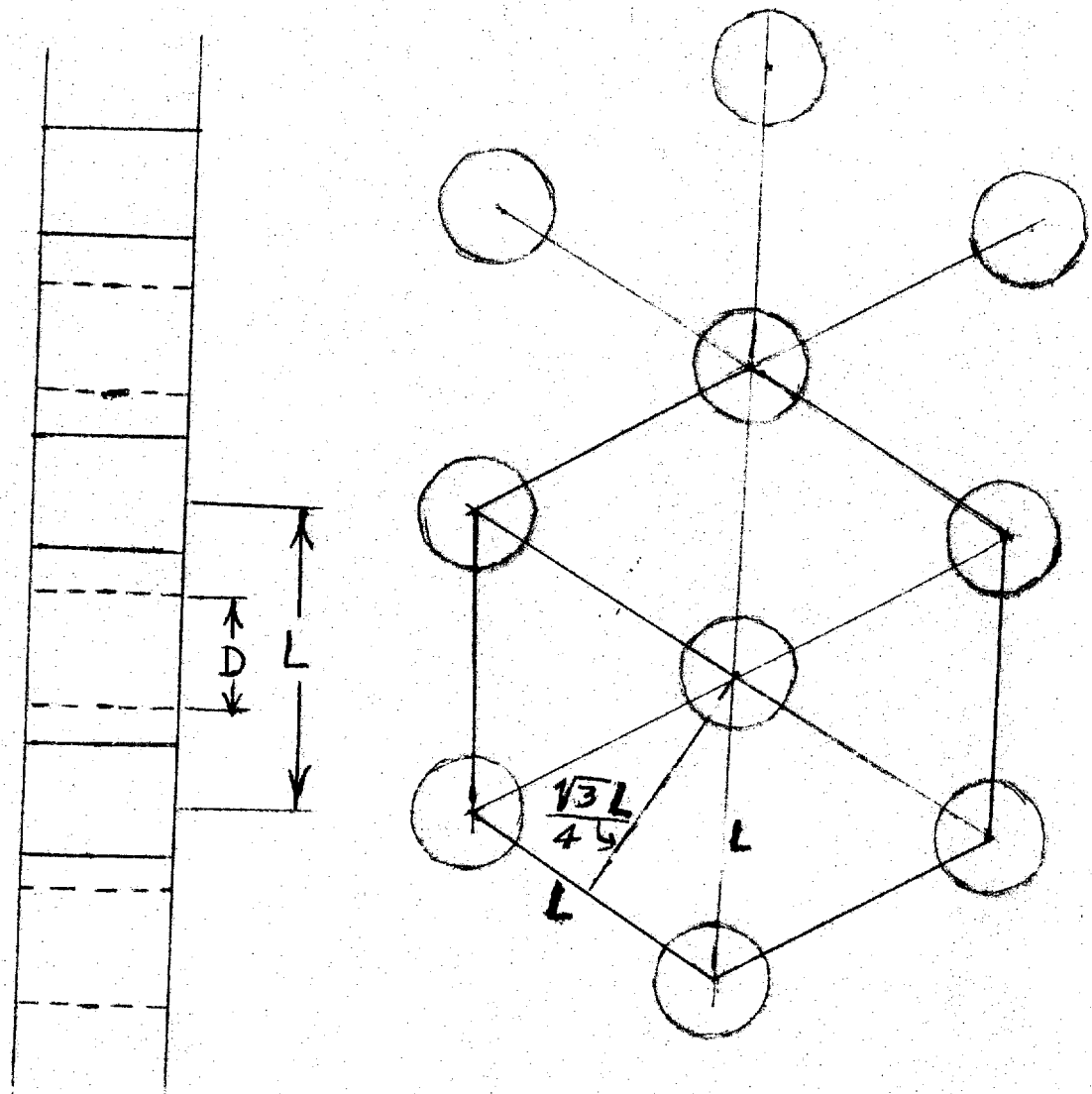


FIGURE 14

shows a rod matrix in a hexagonal pattern and the geometric relations for a given transmittance.

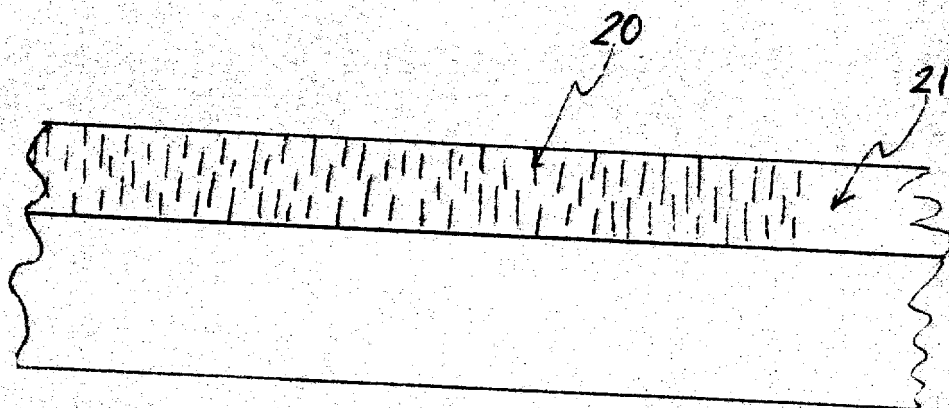


FIGURE 15

shows a photoconductive layer comprising permanently oriented photoconductive dipoles in a plastic matrix on a support.

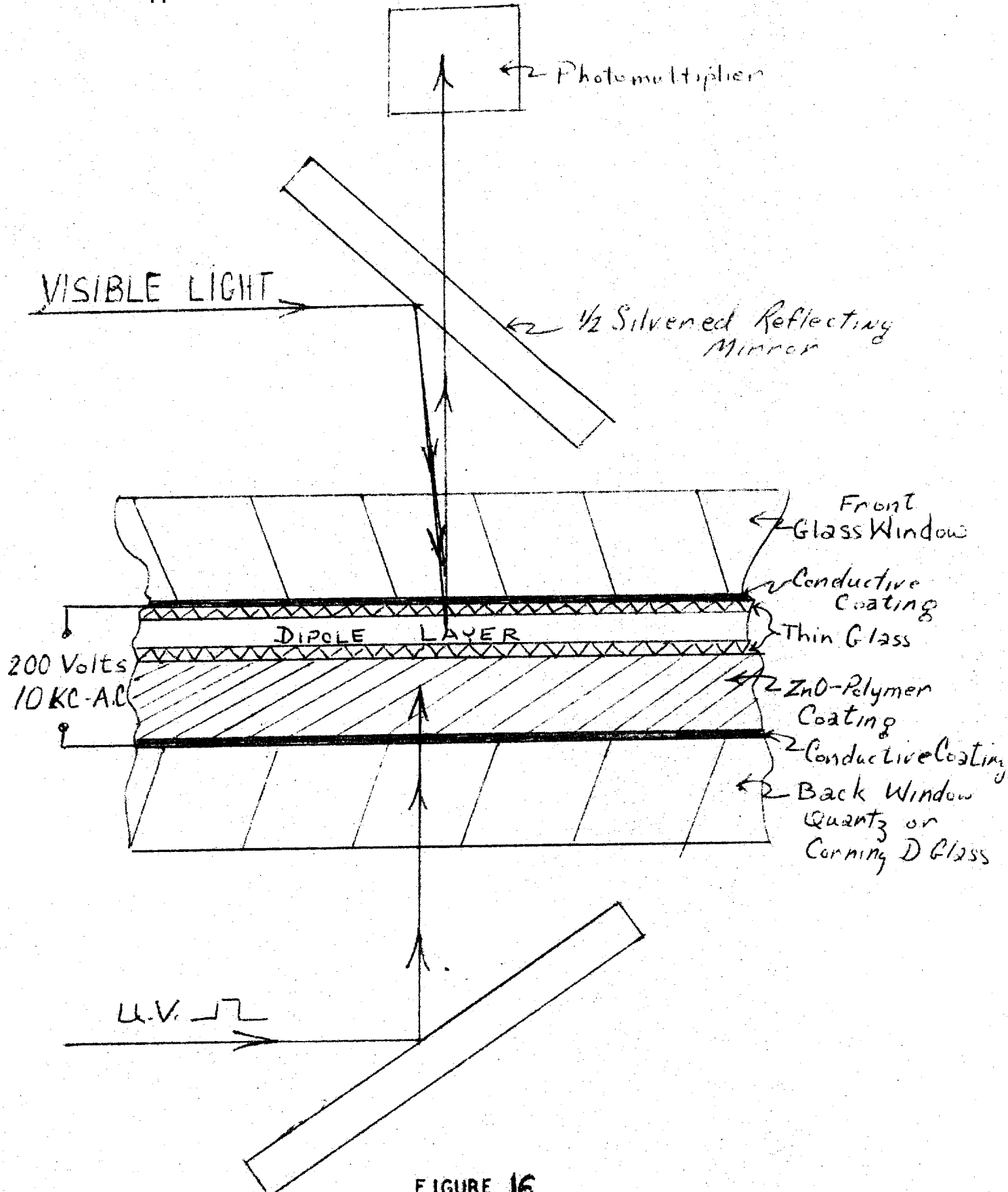


FIGURE 16

shows a combination photoconductive coating and dipole layer actuated by uv light image which is utilized to modulate incident light.

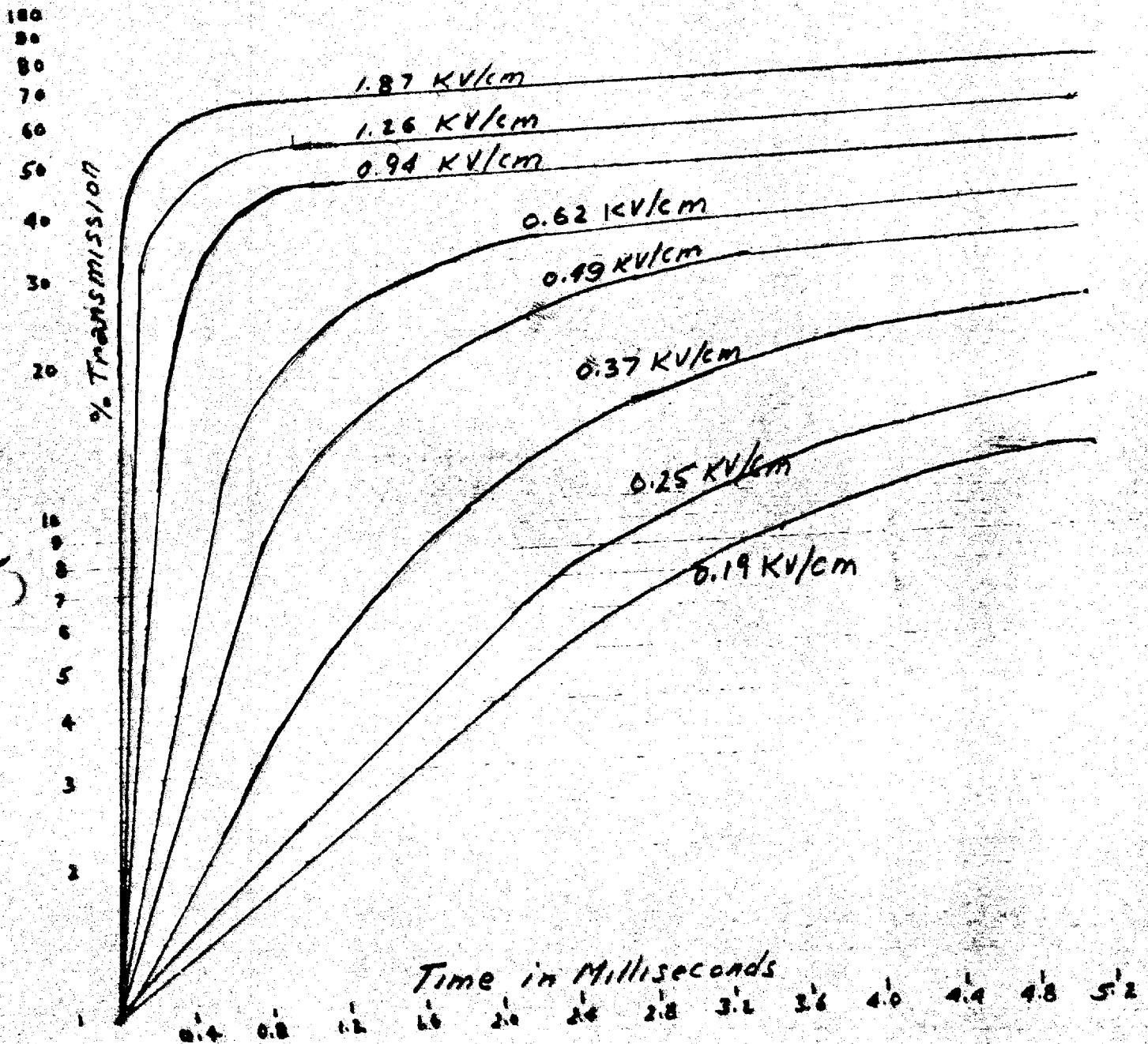


FIGURE 17

shows the transmittance vs. time for various electric field intensities for an herapathite dipole suspension

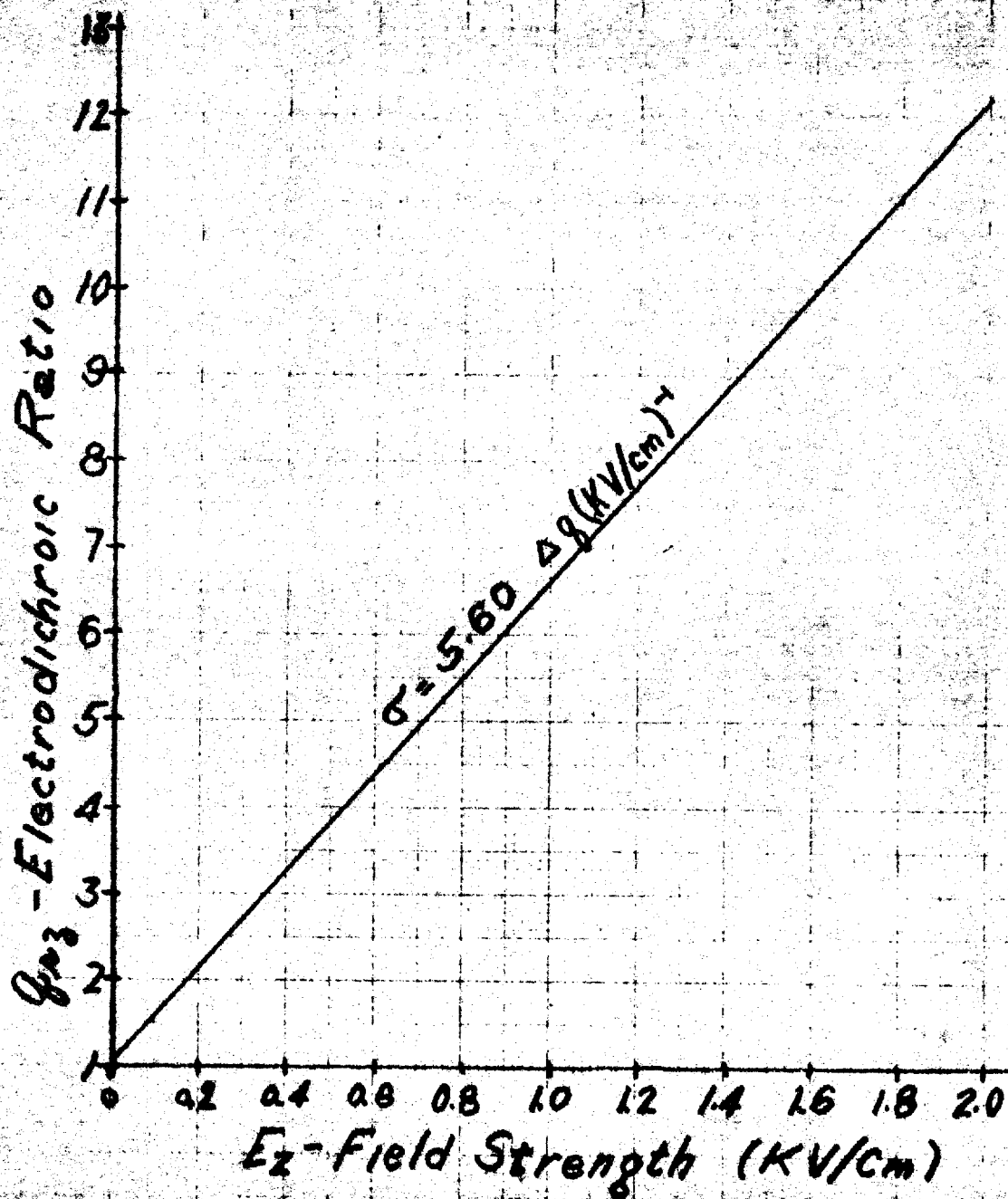


FIGURE 18

shows the random-parallel electrochromic ratio versus electric field strength in kv/cm plotted for an herapathite dipole suspension subjected to an AC pulse.

TAB

August 31st, 1964

STATINTL

PROPOSAL

This proposal relates to the development of a light amplifying screen utilizing dipolar suspension.

1. Description of the Device

The properties of dipole particles in suspension form are described in the enclosed pamphlet entitled "Dipoles and Their Application to Graphic Arts". These dipole suspensions form the basis for the device which is described as follows:

1 is a projector projecting an image in one portion of the spectrum with light 2, which for example may be rich in the ultraviolet or near blue portion of the spectrum. This light source is of a relatively low intensity. The image is projected upon a dipole screen generally indicated as 3, the operation of which is described more fully in connection with Figures 2 and 3.

The projector 4 projects a high intensity light beam 5 through the cutoff filter 6. The function of the cutoff filter 6 is to eliminate the ultraviolet or near blue portion of the spectrum from the light beam 5. The light beam 5 carries no image. A complimentary light cutoff filter 7 is also placed in front of the projector 1 so as to eliminate any light other than the ultraviolet near blue light which is practically invisible.

The dipole screen is constructed as shown in Figures 2 and 3.

Referring to Figure 2, there is shown the condition of the dipole suspension 10 in oriented state, normal to the plane of the screen 3. A neutral molecule 11 is shown just prior to the impingement of an ultraviolet ray 12. After absorbing the ultraviolet ray 12, the neutral molecule 11 splits into positive and negative ions respectively 13 and 14, which migrate to the faces 15 and 16 of the dipole cell under the influence of an electrical field 17 shown in Figure 2.

After the ions 13 and 14 have moved to the cell walls 15 and 16, the electric field 17 is now shielded and the space occupied by the dipole layer 19 is free of the electric field, and the dipole particle 10 in Figure 3 is shown in its random position. The relaxation to the random position occurs by Brownian motion in the field free dipole layer 19.

Thus, in areas which are strongly illuminated by ultraviolet light 12, the dipole particles are disoriented. If the dipole particles 10 are absorbing when disoriented and transparent when oriented, and if the backing layer 20 has a white diffuse reflectivity, then those areas which are illuminated will appear dark, and those areas which are not illuminated will appear white as a result of the reflection of the secondary beam 5 from the projector 4.

Beam 5 carries no image upon incidence but will produce amplified negative image of the projected beam from the projector 1. Therefore, if a film 21 passing through the projector 1 is a negative film, its positive will be produced upon the dipole amplifying screen 3.

Conversely, if reflective dipoles 10 are utilized and the backing screen 20 is a black absorbing screen, then a positive film 21 projected upon the screen 3 and illuminated by the uniform light source 5 will reproduce an amplified positive image.

It will be understood that while the reflective system as shown in Figure 1 requires that the observer's eye be at position 24, that alternatively it will also be possible to utilize a transmittance system where the observer's eye or camera may be located in position 25.

II Work Program

The purpose of the work program will be to establish the feasibility of the above concepts and to set up the equipment essentially as shown in Figure 1.

Projectors 1 and 4 and the filters 6 and 7 are conventional. The dipole screen as shown in Figures 1 and 3 have also been reduced to practical hardware and are demonstrable at the present time and will exhibit a large area uniform change responsive to an applied electric potential.

The work program will concentrate upon, therefore, the study of suitable molecules illustrated as 11 in Figure 2 and incorporated within the layer 19. These molecules will be chosen from well known photochemical species which are capable of being split when subjected to ultraviolet light but which will recombine in the dark.

Numerous such species are known and primarily include transition metal halide salts or the acid halides which will be dissolved within the dipole suspension in such quantity as to be suitable for masking the electric field when illuminated by ultraviolet

light, but which will recombine in the dark.

These studies will initially be performed in laboratory cells and rate studies will be taken of the alignment and disalignment of dipolar materials in the presence of ions combined and uncombined. The rate of disorientation of the dipole particles will be affected by the concentration and the splitting apart of the ions by ultraviolet light and the rate of orientation of the dipoles will depend on the rate of recombination of these ions.

STATINTL

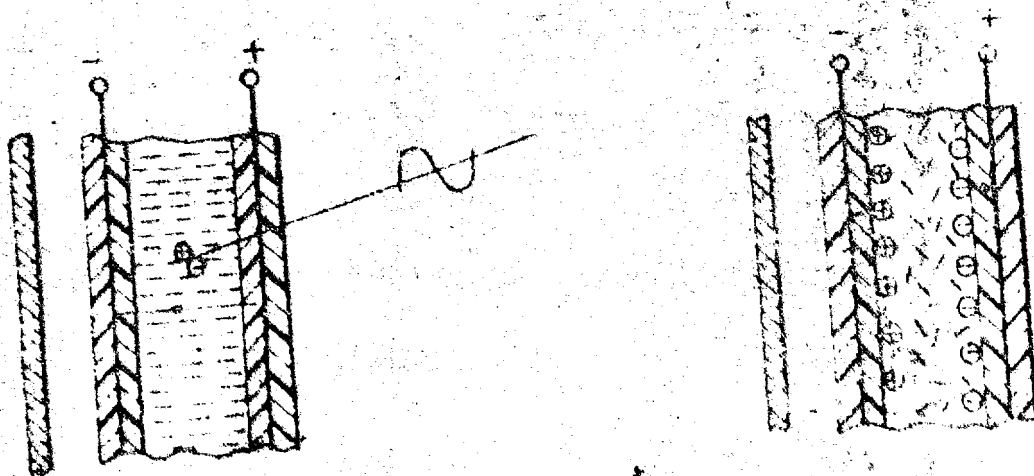
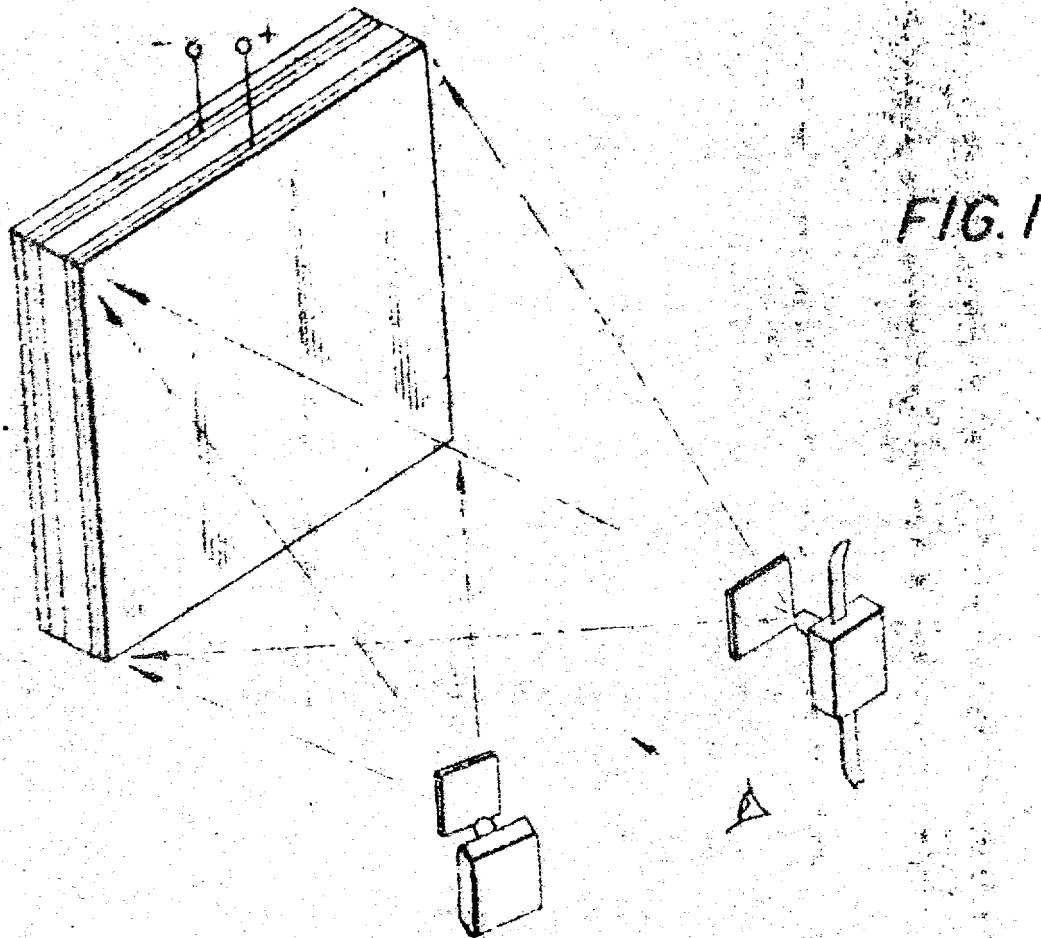
The present equipment which includes a unique optical bench equipped with illuminating source, photosensors, logarithmic amplifiers and memoscope and camera, is essential to the effective prosecution of this work and is already available in operating condition and is presently being utilized part time on other projects. The necessary electrical equipment is also available. Therefore, with only a relatively small expenditure for chemicals and glass ware, we will be able to execute this program with a minimum of delay and only a modest requirement of the purchase of additional equipment.

The work is to be divided into two phases.

Phase I will include the studies of the dipolar photoionic phenomena to establish the necessary parameters.

Phase II will comprise the construction and test of a system shown in Figure 1.

The work on Phase I will continue for six months, but it is hoped that at the end of four or five months progress will be sufficient to make a demonstration based upon Figure 1.



TOPICS TO BE COVERED IN THE FEASIBILITY STUDY OF

A LIGHT AMPLIFYING SCREEN

STATINTL

This contract's main goal is to determine the feasibility of utilizing a dipolar suspension in the development of an advanced rear projection screen. In making this determination certain questions must be answered; some of which are listed below:

1. If a certain level of U-V radiation is required to ionize the molecules, then a higher level must be transmitted through the film because certain losses are incurred at the interfaces of the screen, and due to internal reflections before the radiation reaches the dipolar layer. What is the actual quantum efficiency?
2. What is the attenuation of the original imagery by the screen?
3. What is the selectivity of the Ultraviolet illumination?
4. Will the U-V illumination control the screen to the same degree as it is transmitted by the original; i.e., is the system linear.
5. Will the projected image be as sharp as one on a conventional rear projection screen?
6. Will the ionized material de-ionize with respect to time; furthermore, will its ionizing characteristics vary with age and/or extended use.
7. Will the internal reflection of the U-V, due to the interfaces of the screen affect the presentation.
8. Since the screen is a fluid, there could be thermal gradients due to uneven heating; will this affect the presentation?
9. How will the electric field be controlled?
10. What will the time required for the ions to recombine when the field is released.
11. Is the energy level that is required to pass through the film less than that presently transmitted through the film in conventional rear projection viewers?

12. To what degree will there be migration of the ions over the surface of the screen -- causing blurring of the image -- after the screen has been illuminated?

13. How long can an image be held without any significant loss of quality?

14. Does the energy from the auxiliary illumination affect the dipole suspension? If so, how and to what degree does it affect the output presentation.

15. What will be the quality of the output presentation with respect to:

- a. Modulation Transfer Function
- b. Density range
- c. Density discrimination.

THE VARAD PANEL AND ITS HISTORY

1. History

Everyone is familiar with the TV antennae seen on almost every roof, which are dipoles of large size. The signal strength from such an antenna varies from zero to maximum depending on direction and wavelength.

In the years 1930-1941 [REDACTED]

STATINTL

STATINTL

[REDACTED] the development of polarizing materials, which involves the interaction of light with linear electronically conducting molecular structures.

STATINTL

STATINTL

In 1946, [REDACTED] theorized that a small dipole antenna-like particle would interact with visible light, and that a medium comprising myriads of these antenna-like particles suspended within a fluid would orient in an electric field; thus making possible the variation of light radiation under electrical control.

There is considerable literature over the past 100 years concerning the electro-optical effects of assymetric particles in fluid suspension. However, no electro-optical medium useful for wide-scale application had ever been achieved.

-2-

The concept of the dipole-antennae-particle suspensions gave promise of a solution to the problem of a useful electro-optical medium, and its parameters were predicted from electromagnetic antenna theory. Methods of preparation of dipole suspensions were devised to meet these parameters. Laboratory work on these preparations provided experimental data and prototypes. The VARAD panel was thus created and a new era in electro-optics commenced.

2. Contracts

Following a proposal made to the Navy Department in 1959, a contract was obtained to study the feasibility of utilizing dipolar suspensions in nuclear flash protection.¹ At the same time two other approaches to the nuclear flash protection problem were proposed One approach utilized the electro-optical crystal shutter, and another a self-actuated photothermotropic (VADO) film. Preference was given to the VADO film approach which has been funded by contracts from 1959 to the present time.

The work done on dipoles appeared promising for application to photographic shutters. A contract was subsequently let in 1960 with the Photographic Division of the Bureau of Naval Weapons, Department of the Navy, for a dipole shutter suitable for cameras². While considerable progress was made on this contract, certain problems remained and no follow-on contracts were received.

-3-

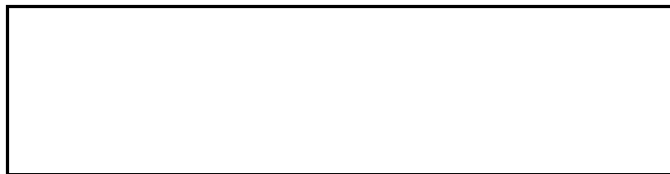
From June 1, 1959 to May 31, 1963, the government funded [redacted] to perform Research and Development in the field of VARAD.

It was the opinion of the management [redacted] [redacted] the VARAD panel was an important development in electro-optics with far reaching consequences, and that additional work would produce a practical result.

Therefore, when the government contracts were not extended, the management [redacted] decided to supply its own funds to further the development of VARAD. From the 1st day of November, 1963, to the 30th day of September, 1964, the corporation in line with this opinion, expended [redacted] on research and prototype development in the field of VARAD. The decision was sound. Breakthroughs achieved within the past year have brought the VARAD panel to a stage of development where it may now be utilized for many applications. This work culminated on October 6, 1964, when a successful 12" x 12" prototype VARAD panel was demonstrated to representatives of the Army, Navy and Air Force. A 24" x 24" VARAD panel was also demonstrated to representatives of the Press on November 30, 1964, to Security Analysts on November 23, 1964, and to representatives of industry on December 2, 1964. As a direct result of these demonstrations, the corporation has obtained government contracts in the field of VARAD [redacted]

STATINTL


STATINTL



TECOM FILMS

TRANSPARENT ELECTRICALLY CONDUCTIVE COATINGS

STATINTL

The TECOM transparent electrically conductive coatings
 are presently available
in laminations only.

Light Transmittance Characteristics

The TECOM film has close to 100% light transmittance from 400-1400 μ , except for usual reflection losses at the air interfaces of the lamination. See graph of Light Transmittance vs. Wavelength from 300-2600 μ .

Electrical Characteristics

The specific resistivity TECOM films, Type TCCA, is approximately 10 ohms-cm.

This coating can be provided most readily in the form of a film approximately 1 mil thick, which has a resistivity of about 4000 ohms per square.

In certain applications where lower resistivities are required, the following Table may be helpful:

-2-

TABLE I

<u>TECOM FILMS</u>	
<u>10 ohm-cm</u>	
<u>TRANSPARENT CONDUCTIVE COATINGS - TYPE TCCA</u>	
<u>Thickness</u> <u>mils</u>	<u>Resistance</u> <u>ohms per square</u>
1.	4000
2.	2000
5.	800
10.	400
20.	200

For resistive heating applications where large current densities are employed, an alternating current is required to avoid electrolytic breakdown at the connecting terminals.

Connecting terminals are embedded in contact with the conductive coating at the edge.

Laminations

Laminations of TECOM film may be made between glass, or plastics such as plexiglass, CR39, and the like.

Uses

Laminates having thin TECOM films are useful for voltage operated devices in which the current requirements are small, and in the microamp to milliamp range. Laminates having thicker TECOM films, or multilayer laminates are useful for resistive heating panels.

-3-

1. Electro-Optic Devices

Electro-optical devices often require highly transparent electrodes to decrease light losses. In such cases TECOM laminates are essential for efficient light transmission.

2. Transparent Resistive Heating Panel

A TECOM laminate having TECOM films a thickness of 0.10" or more, has a resistance small enough to be useful as a heating panel of high visibility with an applied voltage of the order of 100 volts.

Applications include transparent heated windshields, helmets, visors, etc. to reduce fogging and icing.

The application of TECOM laminates as a high transmittance transparent conductor to heated transparent panels maximizes visibility at night or in difficult seeing conditions.

TECOM - Transparent Electrically Conducting Coating

Spectral Transmittance Curve

